Research Square

Preprints are preliminary reports that have not undergone peer review.
They should not be considered conclusive, used to inform clinical practice,
or referenced by the media as validated information.

# Sustainability Linked Assessment of Tropical Soils in Kuppam River Basin, India: Insight into the Geochemistry of Potential Toxic Elements, Source Apportionment and Associated Human Health Risk

**Olin B. Jose**
Government College Kasaragod, Kannur University
**Manoharan A. N**
Government College Kasaragod, Kannur University
**A. Krishnakumar**
drakrishnakumar@gmail.com

National Centre for Earth Science Studies
**K. Anoop Krishan**
National Centre for Earth Science Studies

**Research Article**

**Keywords:** Sustainable Development Goals, Southern Western Ghats, Soil Contamination, Risk Characterization, Hazard Index.

**Posted Date:** November 2nd, 2026

**DOI:** https://doi.org/10.21203/rs.3.rs-11417329/v1

**License:** This work is licensed under a Creative Commons Attribution 4.0 International License.
Read Full License

**Additional Declarations:** No competing interests reported.

# Sustainability Linked Assessment of Tropical Soils in Kuppam River Basin, India: Insight into the Geochemistry of Potential Toxic Elements, Source Apportionment and Associated Human Health Risk

**Olin B. Jose [a,b], Manoharan A. N [b], A.Krishnakumar [a]*, & K. Anoop Krishan [a]**

[a] *National Centre for Earth Science Studies (NCESS), Ministry of Earth Sciences, Govt. of India, Akkulam, Thiruvananthapuram, 695011, Kerala, India.*

[b] *Government College Kasaragod, Vidyanagar, Kerala 671123, India (Kannur University).*

**Corresponding author: drakrishnakumar@gmail.com*

**Keywords:** Sustainable Development Goals, Southern Western Ghats, Soil Contamination, Risk Characterization, Hazard Index.

## Abstract

Soil geochemistry in tropical agricultural catchments reflects interactions among parent material, weathering, land use, and seasonal hydrological processes. This study examined soil geochemistry, contamination levels and sources, and potential human health risks in the Kuppam River Basin. This tropical watershed is prone to contaminant buildup and downstream transport as it transitions from lateritic midlands to mangrove-fringed estuarine lowlands. Soil samples were collected from 42 sampling locations during each season (monsoon and non-monsoon) and analyzed for major oxides and potentially toxic elements (PTEs) using X-ray fluorescence (XRF) spectrometry. Contamination was determined using the geoaccumulation index (Igeo), contamination factor (CF), and the pollution load index (PLI), and the possible health risks were assessed through a human-health risk assessment framework. Soil geochemistry reflected potential contributions from the weathering of Precambrian crystalline parent materials, with possible additional influences from agricultural and other local anthropogenic activities. Positive matrix factorization (PMF) identified potential source signatures consistent with lithogenic and pedogenic processes, along with possible agricultural and other local anthropogenic contributions. The USEPA screening-level risk assessment identified cobalt as the principal contributor to the estimated non-carcinogenic risk and arsenic as the primary carcinogenic concern, with lifetime cancer risks exceeding $10^{-4}$ for both adults and children. Nickel risks remained between $10^{-6}$ and $10^{-4}$, while Pb ingestion risk remained below $10^{-6}$ for both receptors across seasons. Ingestion, dermal contact, and inhalation pathways were considered for As and Ni. Results indicate that small tropical catchments can serve as useful indicators for identifying potential contamination hotspots and prioritizing areas for further assessment and targeted environmental management.

## 1. Introduction

Soil is vital to terrestrial systems; it supports food production, regulates water and nutrient cycles, stores carbon, and helps maintain ecosystem functions. It can act as both a source and a sink for chemical substances; soil geochemistry directly affects soil quality, agricultural productivity, water resources, ecosystem integrity, and human well-being. The accumulation of potentially toxic elements (PTEs) in soil at concentrations above their corresponding background values is a serious environmental issue because of their long persistence, limited degradation, and potential redistribution through erosion, runoff, atmospheric deposition, agricultural practices, and plant uptake(Doran & Zeiss, 2000; Fausak et al., 2024; Kabato et al., 2025; Kopittke et al., 2019; Lal, 2025). These PTEs may come from both geogenic and anthropogenic origins: natural inputs are determined by the weathering of the parent materials, while the use of fertilizers, manure, pesticides, irrigation, and intensive cultivation can alter the concentrations of elements in agricultural soils (Das & Krishnakumar, 2022; Krishnakumar et al., 2021). If PTEs remain enriched in the soil, they may impair the soil's physicochemical properties, affect microbial processes, hinder plant growth, and impact ecosystem functioning. Humans may be exposed through contaminated soil, water, or food; inhalation of particulates; or skin contact, with children generally being particularly susceptible (Y. Wang et al., 2022; Wieczorek et al., 2023). As a result, evaluating PTE contamination must include mapping the spatial distribution and enrichment of these elements, identifying their sources, and assessing potential risks to human health.

These processes are especially significant in tropical areas, where high temperatures, strong chemical weathering, seasonal rainfall, and strong hydrological connectivity can affect the release, transport, and redistribution of

geochemical elements. The Western Ghats (WG), a global biodiversity hotspot, provide a distinctive environment shaped by the interaction of complex rock types, steep topographic gradients, intense monsoonal rainfall, and diverse agricultural and plantation systems, which influence soil development and element mobility (Gadgil, 2011; Kassa et al., 2017; Mgelwa et al., 2025). In the southern part of the Western Ghats, differences in soil and sediment geochemistry have been linked to the lithological features, weathering processes, land use, and human inputs (Gayathri, Krishnan, et al., 2021; Gupta et al., 2024; Krishnakumar et al., 2025; Siji et al., 2025).The area thus provides a suitable natural environment to study how geogenic controls, monsoonal processes, and human activities influence PTE distribution.

A river basin provides a highly useful spatial framework for such an assessment because it integrates lithology, topography, climate, drainage, land use, soil formation, erosion, and hydrological transport within a single connected landscape. Together, these factors influence both the formation of geochemical signatures and the subsequent redistribution of soil-associated elements through runoff, erosion, sediment transport, and deposition. Basin-scale studies can therefore provide a process-based explanation of PTE spatial distribution and help distinguish long-standing geogenic signatures from enrichments caused by land use and anthropogenic inputs(Gayathri, Dev, et al., 2021; Gayathri, Krishnan, et al., 2021; Krishnakumar et al., 2022; Lal, 2012; Reshma & Arunkumar, 2023; Siji et al., 2025). This approach is particularly well suited to humid tropical basins, where seasonal monsoon patterns can modify soil–water interactions and contaminant redistribution.

The Kuppam River Basin (KRB), located in the southern part of WGs, is an example of a coupled environmental system. The basin contains contrasting geological and topographical features, along with diverse land-use practices, including paddy farming, coconut cultivation, arecanut farming, pepper farming, banana farming, and plantation agriculture(KILA, 2015; KSRRC & KSPB, 2023). These environmental gradients influence soil development, element accumulation, and the potential mobility of PTEs. Although previous studies in the Southern Western Ghats have investigated PTE concentrations and contamination, important questions remain regarding how seasonal differences, catchment geology, and land-use pressures jointly influence PTE distributions and potential source signatures, and how these patterns translate into screening-level human-health risks. Addressing these questions requires an integrated assessment that combines seasonal geochemical observations, contamination evaluation, potential-source screening, and health-risk modelling within a catchment framework. Such an approach can strengthen the interpretation of geogenic and potential anthropogenic influences while helping prioritise areas for further investigation and targeted environmental management.

Therefore, this study integrates soil geochemistry, pollutant assessment (including PTEs), source apportionment, and human-health risk evaluation across the KRB. Its specific aims were to: (i) determine the concentrations and spatial distributions of the major oxides and selected PTEs; (ii) assess PTE contamination using the geo-accumulation index (Igeo), contamination factor (CF), and pollution load index (PLI); (iii) identify possible PTE sources through positive matrix factorization (PMF); and (iv) examine the non-carcinogenic and carcinogenic health risks associated with soil exposure. By applying these methods to a monsoon-influenced tropical river basin, the study links element geochemistry to contamination intensity, source contributions, and potential human health effects. This detailed, process-oriented understanding provides a basis for targeted soil monitoring and the sustainable management of agriculture, watersheds, and environmental health in the Western Ghats. The integrated assessment supports evidence-based soil and watershed management, contributing most directly to SDG 15 (Life on Land) through improved understanding of soil geochemistry and PTE distribution, and SDG 3 (Good Health and Well-being) through screening-level evaluation of potential human-health risks. It also supports SDG 6 (Clean Water and Sanitation) indirectly by informing catchment-scale environmental management and identifying areas requiring further investigation.

## 2. Materials and methods

### 2.1 Study area

The Kuppam River Basin (KRB) (**Fig. 1**), a west-flowing interstate river basin, lies along the Southern Western Ghats of India, spanning Karnataka and Kerala. It originates from the Padinalkadu Ghat in Kodagu (Coorg) district at 1,630 m above sea level, flows west through Kerala's Kannur district, and joins the Valapattanam River near Mattul. The river ultimately drains into the Lakshadweep (Arabian) Sea, north of Azhikkal. The basin spans 11.90°–12.18° N and 75.25°–75.35° E, with a drainage area of about 539 km² and a main channel length of approximately 82 km. It exhibits a mainly dendritic drainage pattern, typical of uniform lithological conditions and minimal structural disturbance terrain (CGWB, 2007).

Western Ghats are one of the world's eight "hottest" biodiversity hotspots and a UNESCO World Heritage landscape, recognized for its exceptional ecological and hydrological significance. According to the Western Ghats Ecology Expert report(Gadgil, 2011)the Paithamala hills, which fall within the basin, are classified under ecologically sensitive zone I, indicating the highest level of ecological sensitivity. The basin features rugged highlands in the east that gradually give way to rolling midlands and low-lying coastal plains in the west(*Water Atlas of Kerala*, 1995). The basin has a humid tropical monsoon climate, receiving about 3,800 mm of rainfall yearly, mainly from the Southwest Monsoon (June–September) and partly from the Northeast Monsoon (October–December). Temperatures stay between 24 and 30 °C year-round, with high humidity. The Kuppam River remains perennial because of heavy monsoon rainfall and spring-fed tributaries from the Western Ghats. It supplies water for domestic use, agriculture, inland fisheries, and riparian ecosystems.

A series of riverine villages and settlements such as Kooveri, Therandy, Kuppam, Pattuvam, Payangadi and Mattool further characterize the river course, reflecting the close interaction between the river, agricultural landscapes and downstream settlements (**Table S1**). In recent decades, the Kuppam River Basin has experienced increased human activity due to rapid urbanization, agricultural expansion, and localized waste disposal, particularly downstream(KILA, 2015; KSRRC & KSPB, 2023). These developments have heightened concerns over declining water quality, soil-sediment pollution, and ecosystem well-being, underscoring the need for comprehensive environmental evaluations and sustainable basin management. The present land use/ land cover pattern of the river basin is shown in **Fig. 2**

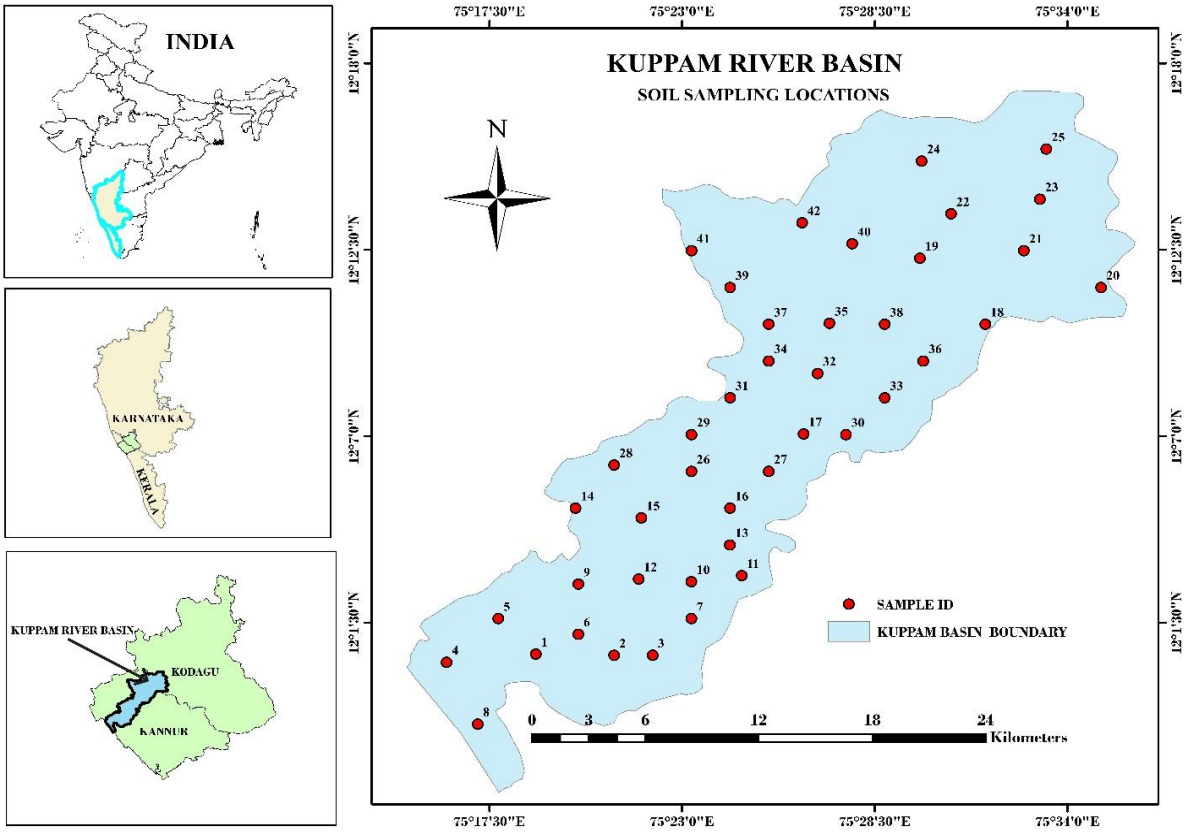



Fig.1 Location map showing the study area with soil sampling locations.

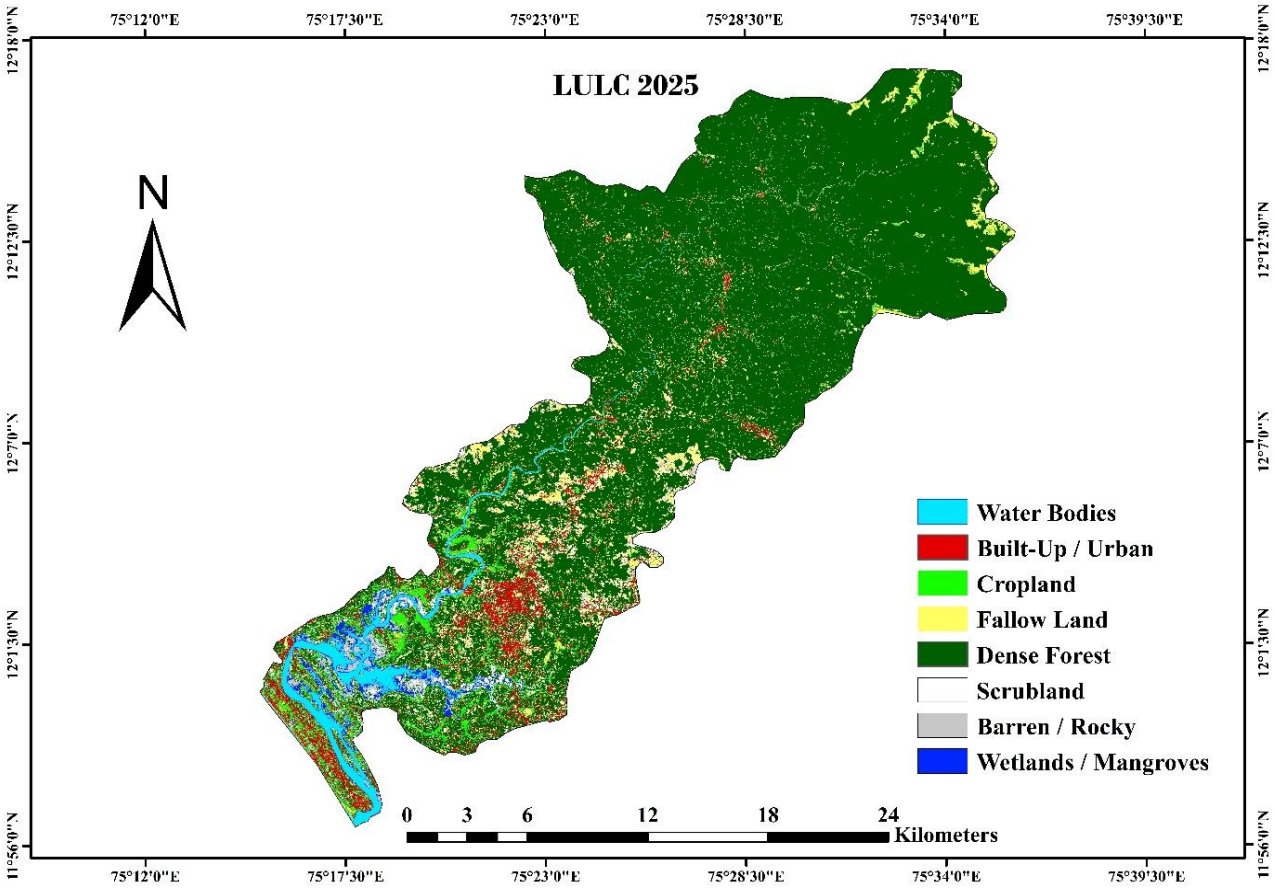



Fig. 2 KRB Land use/land cover (LULC) map

### 2.1.1 Lithology

The Precambrian crystalline rocks that form the foundation of the Kuppam River Basin are part of the Southern Granulite Terrain (SGT), one of the major high-grade metamorphic areas within the Indian Shield (**Fig. 3**). Acidic and intermediate charnockite predominates in the basin and covers the greatest area, especially in the upper and middle sections. These rocks consist of granitoids containing hypersthene and related granulites that have undergone granulite-facies metamorphism, forming the hard basement rock that gives rise to the basin's rugged landscape. The mineral composition of these rocks and their weathering properties have a significant effect on soil development, the course of geomorphological evolution, and the natural geochemical background of the major and trace elements (Nair et al., 2006; Soman, 2023)

In the central and southern parts of the basin, granite gneiss is the main rock type, and laterite is present over a large area of the midland region. This laterite formed through long-term tropical weathering in humid climates, leading to strong leaching of alkali and alkaline earth elements and residual enrichment of iron and aluminum oxides. As a result, lateritic soils occur throughout the basin and are important in controlling the mobility, retention, and bioavailability of potentially toxic elements(de Figueiredo et al., 2025).

Apart from the main lithological units, several minor rock types occur as separate bodies and as narrow linear belts. These include hornblende–diopside gneiss, gray hornblende–biotite gneiss, pyroxene granulite, mica schist, khondalite, banded iron formation (BIF), mylonite, and sillimanite quartzite. These rock types are high-grade metamorphic rocks and zones that have been tectonically deformed during several phases of the crustal evolution of the Southern Granulite Terrain. Although they are small, they contribute significantly to the basin's mineralogical variability and affect the local distribution of Fe, Al, Ti, Mn, and trace metals through differential weathering and mineral decomposition.

Toward the lower part of the basin, the area is a coastal sedimentary environment consisting of sandstone, active channel sand, beach sand, an active beach ridge (made up of fine sand), clayey sand, and clay deposits from old tidal flats. These unconsolidated sediments suggest that Quaternary fluvial, estuarine, and coastal depositional environments existed here, influenced by sea-level changes and sediment reworking along the Malabar Coast. The basin's variety of rock types results from the presence of crystalline basement rocks, lateritic regolith, and unconsolidated coastal sediments. **Table S2** shows the lithology, Mineralogical Composition, and Potential Soil-Forming Implications of KRB.

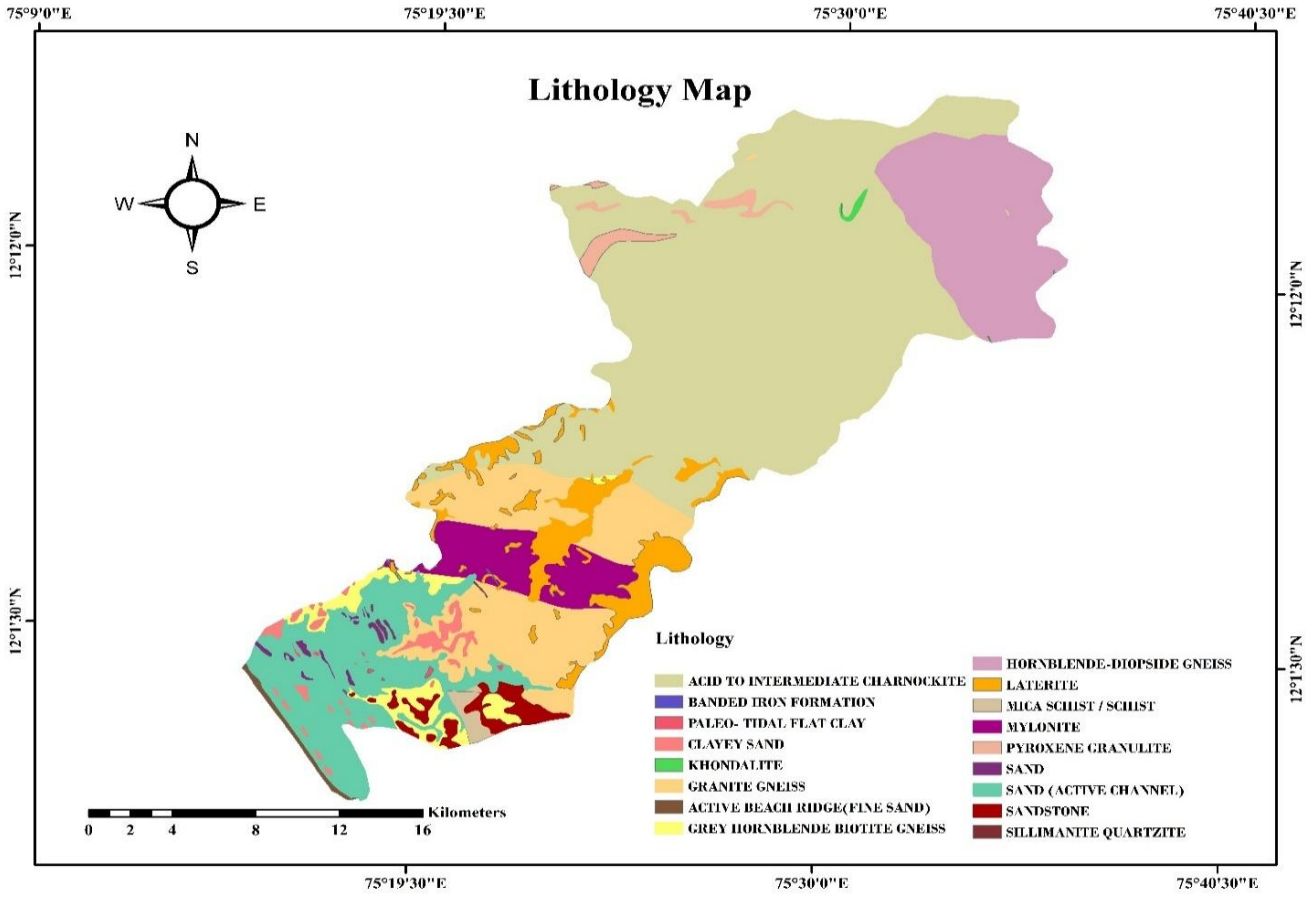



Fig 3. Lithology for the study area (NRSC, 2026).

## 2.2 Sampling and Analytical Methods

To characterize the geochemical properties of the KRB soil, samples are collected systematically. The entire basin is subdivided into 4 × 4 km grid cells using ArcGIS 10.8 software, and at least one sample is collected from each cell based on accessibility, land-use characteristics, and geomorphological conditions. Additional samples are collected from regions with distinct lithologic and geologic formations. Topsoil (0-15 cm, A Horizon) is collected after removing vegetation, litter, and other organic debris and placed in zip-lock polyethylene bags. The geographic coordinates are recorded using a Global Positioning System (GPS). A total of 84 soil samples were collected, comprising 42 samples from each of the monsoon and non-monsoon seasons. Sampling locations were kept consistent between the monsoon and non-monsoon campaigns to facilitate direct seasonal comparison of soil geochemical characteristics. The collected samples were transported to the laboratory. In the laboratory, samples were oven-dried at 60 °C for 48 hours. To maintain sample homogeneity, samples from each location were selected by coning and quartering. The selected samples were gently crushed in an agate mortar and passed through a U.S. Standard Test Sieve (No.230). To prepare pellets for WD–XRF analysis, finely powdered samples were sprinkled over boric acid crystals as a binder in 40 mm aluminum cups and pressed in a 40-ton hydraulic press. The pressed pellets were used for XRF (S8 Tiger and S4

Pioneer, Bruker) analysis, conducted in the XRF laboratory of National Centre of Earth Science Studies (NCESS), Ministry of Earth Sciences, Government of India. SPSS software was used to perform the statistical analysis of the generated data. Descriptive statistics, including minimum, maximum, mean, median, and standard deviation (SD), were calculated. Pearson correlation coefficients (r) were determined separately for the non-monsoon and monsoon data sets to quantify the linear relationships between major-element oxides and potentially toxic elements (PTEs). Seasonal correlation matrices were compared to identify stable associations and changes in magnitude or direction. Significance was assessed at the indicated level($(p<0.05)$). Correlations were taken as evidence for co-variation. The spatial distribution of major ions and potentially toxic elements (PTEs) in the study area was determined using Inverse Distance Weighting (IDW) interpolation in ArcGIS 10.8. This approach estimates values at unsampled locations based on surrounding measurements, weighting them by distance so closer points influence the estimate more than farther points(Shepard, 1968). Separate interpolated layers were created for each major ion and PTE using observed values. IDW was chosen because the measured concentrations were spatially dispersed at discrete sampling locations, and the method offers a simple, deterministic way to represent spatial variation when nearby observations are likely to be more similar.

### 2.3 Quality control and analytical precision

Analytical quality was assessed using certified reference materials MAG and SO1, each analyzed in five replicate measurements (n = 5). **Table 1** presents the XRF analytical quality-control results, including measured and certified concentrations, precision (SD and RSD), and relative error. Accuracy was evaluated by comparing measured concentrations with certified values, while precision was assessed using standard deviation (SD) and relative standard deviation (RSD). RSD was calculated as:

$$RSD\ (\%)\ =\ (SD\ /\ Mean)\ \times\ 100 \quad (1)$$

$$Relative\ Error\ (\%) = \left|\frac{(Measured - Certified)}{Certified}\right| \times\ 100 \quad (2)$$

Table 1: Certified Reference Values and Quality Control Measurements for MAG and SO1 Standards ($n = 5$)

| Element | Unit | Measured Average Value (n = 5) | Certified Reference Value | Standard Deviation (SD) | Relative SD (%) | Relative Error (%) |
|---|---|---|---|---|---|---|
| **$SiO_2$** | % | 48.98 | 50.40 | 0.22 | 0.45 | 2.82 |
| **$Al_2O_3$** | % | 15.82 | 16.40 | 0.06 | 0.38 | 3.54 |
| **Total Fe as $Fe_2O_3$** | % | 6.81 | 6.80 | 0.015 | 0.22 | 0.15 |
| **MnO** | % | 0.096 | 0.10 | 0.01 | 10.42 | 4.00 |
| **MgO** | % | 2.97 | 3.00 | 0.014 | 0.47 | 1.00 |
| **CaO** | % | 1.36 | 1.37 | 0.000 | 0.00 | 0.73 |
| **$Na_2O$** | % | 3.84 | 3.83 | 0.012 | 0.31 | 0.26 |
| **$K_2O$** | % | 3.61 | 3.55 | 0.008 | 0.22 | 1.69 |
| **$TiO_2$** | % | 0.74 | 0.75 | 0.005 | 0.68 | 1.33 |
| **$P_2O_5$** | % | 0.17 | 0.16 | 0.000 | 0.00 | 6.25 |
| **V** | ppm | 132.10 | 140.00 | 0.34 | 0.26 | 5.64 |

| | | | | | | |
|---|---|---|---|---|---|---|
| **Pb** | ppm | 18.80 | 20.00 | 0.20 | 1.06 | 6.00 |
| **Ni** | ppm | 54.20 | 53.00 | 0.48 | 0.89 | 2.26 |
| **Co** | ppm | 24.30 | 25.00 | 0.22 | 0.91 | 2.80 |
| **Cr** | ppm | 96.10 | 97.00 | 0.42 | 0.44 | 0.93 |
| **Cu** | ppm | 32.80 | 30.00 | 1.37 | 4.18 | 9.33 |
| **Zn** | ppm | 128.63 | 130.00 | 0.45 | 0.35 | 1.05 |
| **As** | ppm | 11.50 | 12.00 | 0.11 | 0.96 | 4.17 |

**Note:** *n* = number of replicate measurements.

### 2.4 Assessment of Potentially Toxic Element Contamination

Soil contamination is assessed using pollution indices such as the Geoaccumulation Index (Igeo), Contamination Factor (CF), and Pollution Load Index (PLI)(Hakanson, 1980; Muller, 1969; Tomlinson et al., 1980). These indices require a geochemical background value. The background value (Bn) represents the natural compositional and mineralogical concentrations of specific metals in an undisturbed or parent source. For the calculation of geochemical indices, the Bn value is derived using a hybrid reference approach. Element-specific baseline values reported by Krishnakumar et al., 2022 for soils of the Periyar River Basin in the southern Western Ghats were adopted where corresponding data were available. For elements not covered in that study, reference concentrations from the upper continental crust (UCC) were used(Rudnick & Gao, 2003).The selected background concentration for each element was applied consistently in calculating the contamination factor and geoaccumulation index. Igeo assessed the level and degree of contamination for individual elements, and CF was used to investigate element enrichment and infer potential anthropogenic contributions relative to natural geochemical controls. PLI was used to describe the overall multi-element contamination and pollution burden at sampling sites. Ranges and categories used in the contamination study are incorporated in **Table S3**

***Geoaccumulation Index:*** The concept of the geoaccumulation index *(Igeo*) is put forward by (Muller, 1969) to determine heavy metal concentrations. This index is classified into seven grades or classes, with index classes ranging from 0-6.

$$Igeo = Log2\left[\frac{Cn}{1.5Bn}\right] \quad (3)$$

$C_n$ concentration of specific individual heavy metal, $B_n$(ppm) - value of geochemical background and 1.5 a constant.

***Contamination factor:*** The Contamination Factor is an index that consists of a single element and is used to assess the degree of contamination in the soil at a particular site due to that individual element(Muller, 1969). It is the ratio of the concentration of a particular metal in the soil to the corresponding regional background level, as given by the equation below:

$$CF = \frac{\text{Cn Sample}}{\text{Cn Background}} \quad (4)$$

***Pollution Load Index (PLI)***: The Pollution Load Index (PLI) provides an integrated assessment of the overall level of soil pollution by combining the contamination factors of all analyzed elements(Tomlinson et al., 1980).

$$PLI = \sqrt[n]{\left(C_{f_1} \times C_{f_2} \times C_{f_3} \times \ldots\ldots\ldots \times C_{f_n}\right)} \quad (5)$$

## 2.5 Human Health Risk Assessment

The potential human health risks from exposure to potentially toxic elements (PTEs) in soils of the Kuppam River Basin were assessed using the risk evaluation framework recommended by the United States Environmental Protection Agency (USEPA, 1989, 2011). The main exposure routes for soil are ingestion, skin contact, and inhalation of airborne particles. Separate assessments were conducted for adults and children.**Table S4** explains the classification criteria used for the human health risk assessment study. **Tables S5 and S6** detail the exposure parameters, toxicological reference values, and exposure constants used for the human health risk assessment of potentially toxic elements in soils.

### 2.5.1 Non-Carcinogenic Risk Assessment

The equations for calculating the average daily dose (ADD) through soil ingestion, dermal absorption, and inhalation are as follows;

$$Soil\ ingestion, ADD\ ing = C \times \frac{Ing\ R \times EF \times ED}{BW \times AT} \times 10^{-6} \quad (6)$$

where:

C = concentration of the element in soil (mg $kg^{-1}$),IngR = soil ingestion rate (mg $day^{-1}$), EF = exposure frequency (days $year^{-1}$), ED = exposure duration (years), CF = conversion factor ($10^{-6}$ kg $mg^{-1}$), BW = body weight (kg), AT = averaging time (days)

$$Inhalation, ADD\ inh = C \times \frac{Inh\ R \times EF \times ED}{PEF \times BW \times AT} \quad (7)$$

where:

InhR = inhalation rate ($m^3$ $day^{-1}$), PEF = particle emission factor ($m^3$ $kg^{-1}$)

$$Dermal\ contact, ADD\ derm = C \times \frac{SA \times AF \times ABF \times EF \times ED}{BW \times AT} \times 10^{-6} \quad (8)$$

where:

SA = exposed skin surface area ($cm^2$), AF = soil adherence factor (mg $cm^{-2}$), ABS = dermal absorption factor (unitless)

The hazard quotient is the ratio of the sum of the average daily dose (ADD) to the chronic reference dose (RfD). It is calculated by comparing exposure to a material with a reference value for toxicity. It is a unitless number typically used to estimate potential non-carcinogenic risk.

$$HQ = \frac{ADD(Ingestion \times Inhalation \times Dermal)}{RfD} \quad (9)$$

The health index (HI) is the sum of hazard quotients for all individual elements. It is calculated by

$$HI = \sum HQ = HQ\ ing + HQ\ inh + HQ\ derm \quad (10)$$

If HI is less than 1, there is no significant health risk, and the exposure is safe. If HI is greater than 1, a significant health risk exists.

### 2.5.2 Carcinogenic Risk Assessment

The lifetime carcinogenic risk associated with exposure to carcinogenic PTEs was estimated using the USEPA methodology. The carcinogenic risk (CR) for each exposure pathway was calculated as follows:

$$LCR = ADD(\ ingestion, inhalation, dermal) \times CSF \quad (11)$$

Where CSF is the cancer slope

If LCR< $10^{-6}$, LCR>1× $10^{-4}$, and LCR 1× $10^{-6}$ to 1× $10^{-4}$ signify tolerable danger to humans, high risk of cancer development, and no carcinogenic risk, respectively.

$$TCR = \sum cancer\ risk = cancer\ risk_{ing} + cancer\ risk_{inh} + cancer\ risk_{derm} \quad (12)$$

### 2.6 Positive Matrix Factorization (PMF)

Positive Matrix Factorization (PMF) is a multivariate receptor model to determine the quantity and sources of environmental contaminants. It was developed by (Paatero, 1997; Paatero & Tapper, 1993, 1994).EPA PMF 5.0 to investigate the potential sources and geochemical controls of potentially toxic elements (PTEs).

The U.S. Environmental Protection Agency (USEPA) recommended this method for source apportionment. Unlike conventional pollution indices, which mainly focus on the level and extent of contamination, PMF calculates contributions from geogenic and anthropogenic sources without requiring predefined source profiles, increasing the reliability of source identification. By accounting for measurement uncertainties and applying non-negativity constraints, the model improves the robustness and physical interpretability of the results. Because of this, PMF is especially appropriate for tropical agricultural catchments, as potentially toxic elements (PTEs) may come from a variety of sources such as bedrock weathering, agricultural inputs, atmospheric deposition, and other anthropogenic activities. Since it allows the relative contribution of these sources to be determined, PMF supplements the contamination indices and offers a process-based understanding of PTE accumulation, thus aiding targeted pollution management and sustainable environmental planning at the catchment scale (Sun et al., 2020; D. Wang et al., 2009).In the present dataset, all 18 elements in the 42 soil samples were reported to be above their respective analytical detection limits, with no missing observations. All are classified as strong variables, with signal-to-noise ratios ranging from 3.5 to 9.0.

The formulas used in the study are as follows:

$$x_{ij} = \sum_{K=1}^{p} g_{ik} f_{kj} + e_{ij} \quad (13)$$

where $x_{ij}$is the concentration of the $j^{th}$chemical species in the $i^{th}$sample; $g_{ik}$is the contribution of the $k^{th}$source to the $i^{th}$sample; $f_{kj}$is the concentration of the $j^{th}$species in the $k^{th}$source profile; $e_{ij}$is the residual; and $p$is the total number of factors.

$$Q = \sum_{\{i=1\}}^{\{n\}} \sum_{\{j=1\}}^{\{m\}} \left(\frac{e_{ij}}{u_{ij}}\right)^2 \quad (14)$$

where $u_{ij}$is the uncertainty associated with the measured concentration.

*For concentrations greater than the MDL:*

$$u = \sqrt{\left(EF \times C\right)^2 + \left(\frac{MDL}{2}\right)^2} \quad (15)$$

*where $C$is the measured concentration, MDL is the method detection limit, and $EF$is the analytical error fraction.*

Separate seasonal PMF analyses were performed on the non-monsoon and monsoon datasets(42 samples per season). Models with different numbers of factors were tested to select one that balanced goodness of fit, residual behavior, repeat run convergence, and geochemical interpretability. Model performance was evaluated based on available statistics of the objective function, uncertainty-scaled residuals, and observed-vs-predicted concentrations. Numerical reproducibility was checked by 20 independent base runs with different random seeds. The rotational sensitivity was also studied using a Fpeak transform with strength 0.5. Resolved factors were interpreted according to their elemental profiles, regional geological setting, seasonal correlation patterns, and available land-use information.

## 3 Results and discussion

### 3.1 Demographic Dynamics in Kuppam River Basin

The population of the KRB grew by approximately 59.0%, increasing from 195,430 in 1981 to 310,756 in 2011 (**Table 2**). This growth was accompanied by a gradual shift in the rural–urban structure. The rural population increased gradually from 145,210 to 208,994, a 43.9% increase, while the urban population grew rapidly from 50,220 to 101,762, a 102.6% increase. As a result, the urban share rose from 25.7% in 1981 to 32.7% in 2011, while the rural share fell from 74.3% to 67.3%. Thus, the rapid increase in the urban population indicates progressive settlement expansion and changing land-use pressure in the basin.

These demographic changes provide an important socio-economic context for interpreting spatial variations in soil geochemistry. Agricultural intensification, fertilizer and agrochemical application, irrigation, settlement expansion, domestic waste, wastewater, construction activities, and atmospheric deposition can affect soil elemental concentrations(Al-Shammary et al., 2024; De Corato et al., 2024; X. Wang et al., 2025). These activities may contribute to the accumulation of PTEs, including Cd, Pb, Cr, Ni, Cu, and Zn (Wei et al., 2024).

Table 2. Demographic profile of the Kuppam River Basin based on the Population Census(Office of the Registrar General & Census Commissioner, 1982, 1991, 2001, 2011)

| **Demographic Metric** | **1981** | **1991** | **2001** | **2011** |
|---|---|---|---|---|
| **Total Population** | 195,430 | 254,410 | 296,720 | 310,756 |
| **Male Population** | 97,310 | 129,140 | 154,580 | 162,013 |
| **Female Population** | 98,120 | 125,270 | 142,140 | 158,143 |
| **Rural Distribution** | 145,210 | 181,900 | 200,120 | 208,994 |
| **Urban Distribution** | 50,220 | 72,510 | 96,600 | 101,762 |

### 3.2 Geochemistry of major oxides

Surface soils in the Kuppam River Basin showed substantial spatial variability but relatively limited seasonal differences in major-oxide composition (**Table 3; Fig. 4**), suggesting that lithological variability and weathering processes exert a stronger control on soil geochemistry than seasonal monsoonal fluctuations. In each season, the major oxides appear in the order $SiO_2 > Al_2O_3 > Fe_2O_3 > TiO_2 > MgO > CaO > K_2O > Na_2O > P_2O_5 > MnO$. This is comparable with Periyar soil(Krishnakumar et al., 2022): $SiO_2$ was the dominant major oxide, ranging from 26.64 to 54.14 wt% (mean: 42.70 wt%) during the non-monsoon season and from 33.08 to 54.09 wt% (mean: 42.21 wt%) during the monsoon season.The relatively high spatial variability of $SiO_2$ (SD = 4.84 and 4.57 wt% respectively) when compared with that of MnO (≤0.07 wt%) and $P_2O_5$ (0.04 wt%) is due to the heterogeneous parent materials in the basin(Conley, 2002).The average concentrations of $Al_2O_3$ (25.65–26.12 wt%) and $TiO_2$ (1.50–1.53 wt%) . Total iron, measured as $Fe_2O_3$, amounts to 12.79–12.93 wt%. $Al_2O_3$, $TiO_2$, and $Fe_2O_3$ are retained and have accumulated as residual components during the intense chemical weathering, which is in line with the development of ferrallitic soils(Cornu et al., 2009; Fritsch et al., 2005; Middelburg et al., 1988).On the other hand, MgO, CaO, $Na_2O$, and $K_2O$ are strongly depleted as compared to their respective UCC values of 2.48, 3.59, 3.27, and 2.80 wt% ,reflecting the leaching of alkali and alkaline earth elements during prolonged weathering.The slight enrichment of $P_2O_5$ (0.26–0.27 wt%) and MnO (~0.13 wt%) when compared to their UCC values of 0.15 and 0.10 wt%, respectively, indicates that these elements have been relatively retained or associated with secondary mineral phases. Taken as a whole, the major-oxide composition reveals intense chemical weathering, involving a marked depletion of the base cations and a residual enrichment of the Al–Fe–Ti-bearing phases, which is in agreement with the development of kaolinitic to ferrallitic soils(Bernal et al., 2006; Fritsch et al., 2005).

Table 3. Descriptive statistics of major oxide concentrations (wt.%) in surface soils for the nonmonsoon and monsoon seasons of the Kuppam River Basin

| | **Nonmonsoon** | | | | **Monsoon** | | | | **UCC value**(Rudnick & Gao, 2003) | **Periyar Basin (Combined Average)**(Krishnakumar et al., 2022) |
|---|---|---|---|---|---|---|---|---|---|---|
| **Major oxides (wt %)** | **Maximum** | **Minimum** | **Average** | **SD** | **Maximum** | **Minimum** | **Average** | **SD** | | |
| **$SiO_2$** | 54.14 | 26.64 | 42.7 | 4.84 | 54.09 | 33.08 | 42.21 | 4.57 | 66.6 | 50.25 |

| | | | | | | | | | | |
|---|---|---|---|---|---|---|---|---|---|---|
| **$Al_2O_3$** | 30.75 | 20.52 | 25.65 | 2.19 | 31.51 | 20.46 | 26.12 | 2.44 | 15.4 | 25.65 |
| **Total Fe as** $Fe_2O_3$ | 22.79 | 7.66 | 12.93 | 3.28 | 19.9 | 6.74 | 12.79 | 2.85 | 5.04 | 12.79 |
| **Total Mn as MnO** | 0.27 | 0.03 | 0.13 | 0.05 | 0.33 | 0.02 | 0.13 | 0.07 | 0.1 | 0.13 |
| **MgO** | 1.67 | 0.52 | 1.13 | 0.28 | 1.66 | 0.59 | 1.07 | 0.22 | 2.48 | 1.33 |
| **CaO** | 1.76 | 0.28 | 0.87 | 0.4 | 1.52 | 0.3 | 0.78 | 0.33 | 3.59 | 1.08 |
| **$Na_2O$** | 0.87 | 0.05 | 0.33 | 0.21 | 0.99 | 0.11 | 0.26 | 0.15 | 3.27 | 0.85 |
| **$K_2O$** | 1.3 | 0.4 | 0.81 | 0.21 | 2.09 | 0.54 | 0.83 | 0.28 | 2.8 | 1.89 |
| **$TiO_2$** | 2.21 | 1.06 | 1.53 | 0.28 | 2.23 | 1.06 | 1.5 | 0.28 | 0.64 | 1 |
| **$P_2O_5$** | 0.4 | 0.21 | 0.27 | 0.04 | 0.35 | 0.18 | 0.26 | 0.04 | 0.15 | 0.28 |

338

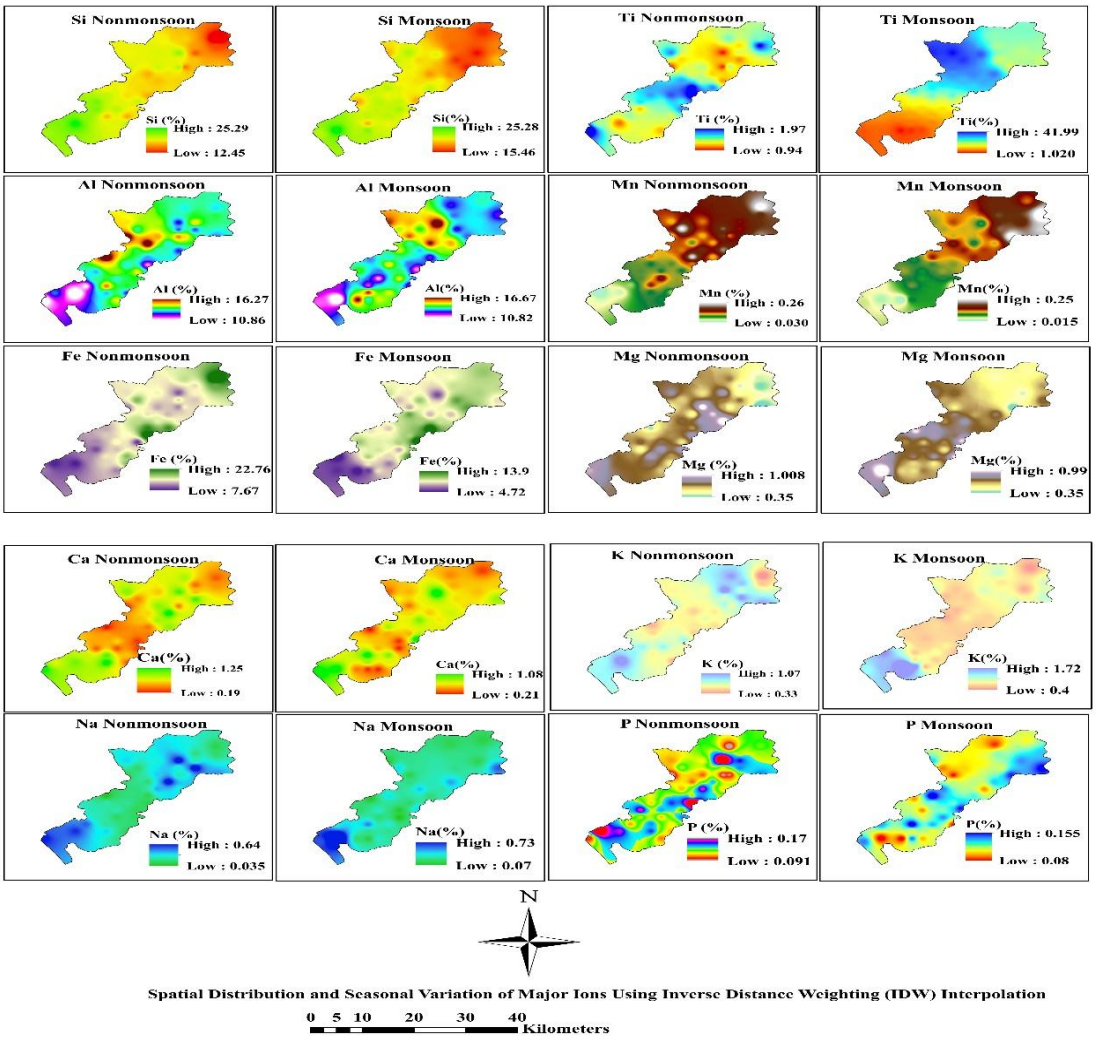



Fig 4. Spatial interpolation maps of major ion concentrations during the non-monsoon and monsoon seasons

### 3.3 Potential toxic elements

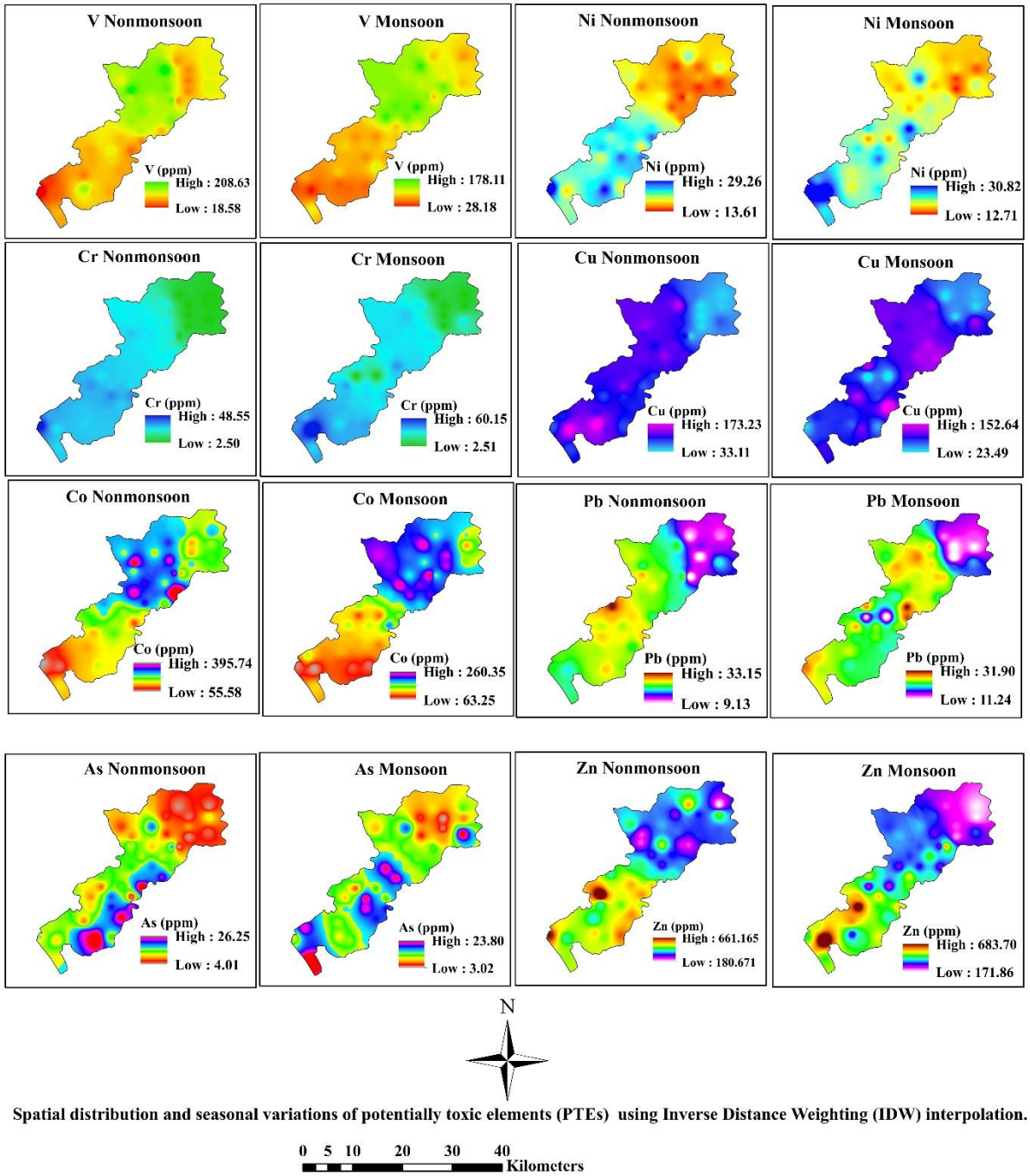
The concentrations of potentially toxic elements (PTE) in the surface soils of the Kuppam River Basin are given in **Table 4**, while their spatial distributions are illustrated in **Fig. 5**. The elements studied show considerable spatial variability, but their mean abundance ranks in the same order in both seasons: Zn > Co > V > Cu > Pb > Cr > Ni > As. Zn is the most abundant PTE, with mean concentrations of 382.12 ppm in the non-monsoon season and 365.44 ppm in the monsoon season; Co follows at 170.88 and 161.90 ppm, respectively, followed by V at 108.06 and 103.41 ppm, and Cu at 91.64 and 82.26 ppm. In contrast, Cr (22.38–22.79 ppm), Pb (19.11–23.53 ppm), Ni (19.15–23.63 ppm), and As (11.18–11.30 ppm) occur at much lower concentrations. Zn and Co showed pronounced spatial variability but limited seasonal differences, indicating localized and temporally stable enrichment. Relative to Upper Continental Crust (UCC) values, Co, Zn, and Cu were markedly enriched, likely reflecting mixed lithogenic and anthropogenic influences. The mean concentration of Co (~166 ppm) is about 9.6 times its UCC value (17.3 ppm), and that of Zn (~373 ppm) is approximately 5.6 times its UCC value (67 ppm), while the concentration of Cu (~87 ppm) is about three times its UCC value (28 ppm). Agricultural inputs, particularly fertilizers (phosphate-based) and organic manures, contribute to Zn and Cu enrichment, whereas mineral weathering likely exerts stronger control on Co(Luo et al., 2025). As (~11 ppm) is moderately enriched relative to its UCC value of 4.8 ppm, whereas Pb (~21 ppm) is only slightly enriched relative to its UCC value of 17 ppm. In contrast, Cr (~22.5 ppm) and Ni (~21.4 ppm) are strongly

depleted relative to UCC values of 92 and 47 ppm, respectively, which may be attributable to the geochemical features of the parent material and differential mobility during weathering(Middelburg et al., 1988; Sababa et al., 2021). V (~105 ppm) remains close to its UCC value (97 ppm), showing only limited fractionation. Overall, the distribution of PTEs results from the combined effects of parent-rock composition, weathering-driven redistribution, and local anthropogenic inputs. The comparative data in **Table 5** provide further context for these patterns by referring to regional and global soil compositions.

Agricultural activities are an important potential source of diffuse anthropogenic inputs within the Kuppam River Basin, with temporal variations in cultivated area and major-crop production indicating changing intensity and spatial extent of agricultural land use (**Table 6**). Fertilizer and agrochemical use can enhance the mobilization and redistribution of nutrient and trace-element inputs through surface runoff, erosion, and leaching, particularly during monsoon conditions. Fertilizer-consumption data for Kannur indicate substantial agricultural input intensity in the region (**Table 7**), while state-level data further show widespread use of chemical pesticides across Kerala (**Table 8**). As shown in **Fig. 6**, fertilizer consumption in Kannur varied annually during 2021–2026, with urea and MOP consistently representing the largest inputs.

Table 4**.** Potentially toxic element (PTE) concentrations in the surface soils of the Kuppam River Basin during the non-monsoon and monsoon seasons

| **Potentially Toxic Elements** | **Non-Monsoon Maximum** | **Non-Monsoon Minimum** | **Non-Monsoon Average** | **Non-Monsoon SD** | **Monsoon Maximum** | **Monsoon Minimum** | **Monsoon Average** | **Monsoon SD** | **UCC Value (ppm)** |
|---|---|---|---|---|---|---|---|---|---|
| **V (ppm)** | 208.77 | 18.45 | 108.06 | 42.15 | 178.12 | 28.14 | 103.41 | 40.14 | 97 |
| **Pb (ppm)** | 33.13 | 9.10 | 23.53 | 5.13 | 31.92 | 11.20 | 23.63 | 5.46 | 17 |
| **Ni (ppm)** | 29.29 | 13.61 | 19.11 | 3.68 | 30.83 | 12.70 | 19.15 | 3.99 | 47 |
| **Co (ppm)** | 395.86 | 55.47 | 170.88 | 68.96 | 260.46 | 63.18 | 161.90 | 57.51 | 17.3 |
| **Cr (ppm)** | 48.60 | 2.50 | 22.38 | 10.65 | 60.19 | 2.50 | 22.79 | 11.46 | 92 |
| **Cu (ppm)** | 173.28 | 33.00 | 91.64 | 31.14 | 152.89 | 23.40 | 82.26 | 26.55 | 28 |
| **Zn (ppm)** | 1154.08 | 180.40 | 382.12 | 156.12 | 1280.00 | 171.80 | 365.44 | 177.68 | 67 |
| **As (ppm)** | 26.29 | 4.00 | 11.18 | 5.61 | 23.81 | 3.00 | 11.30 | 4.88 | 4.8 |




**Spatial distribution and seasonal variations of potentially toxic elements (PTEs) using Inverse Distance Weighting (IDW) interpolation.**

Fig.5 Spatial interpolation maps of potentially toxic element concentrations during the non-monsoon and monsoon season

Table 5 Assessment of PTEs concentrations in the present study in relation to concentrations reported in other studies

| SL No. | Basin | V | Pb | Ni | Co | Cr | Cu | Zn | As | Refernces |
|---|---|---|---|---|---|---|---|---|---|---|
| 1 | Kuppam Basin, Kerala (Present Study) | 105.74 | 23.58 | 19.13 | 166.39 | 22.59 | 86.95 | 373.78 | 11.24 | Present St |
| 2 | Tigris River Basin (Mesopotamia) | 42.5 | 68.4 | 45.2 | 18.9 | 92.1 | 51.3 | 120.4 | 14.2 | (AI-Shaw 2022) |
| 3 | Katanga Basin (Dem. Rep. of Congo) | 35.1 | 215.6 | 134 | 88.5 | 110.2 | 450.8 | 325 | 22.8 | (Wieczore 2023) |
| 4 | Datong Basin (North China) | 65 | 26.5 | 29.8 | 14.2 | 62.3 | 31.5 | 78.2 | 48.6 | (Wu et al. |
| 5 | Balkhash Basin (Kazakhstan) | 39.8 | 185.3 | 52.1 | 24.3 | 128.4 | 180.5 | 410.2 | 25.1 | (Madibek 2023) |
| 6 | Kallada River Basin, Kerala | — | 15.2 | 18.4 | 12.1 | 48.6 | 38.3 | 54.1 | — | (Mohan Krishnaku |
| 7 | Karamana River Basin, Kerala | — | 18.5 | 22.1 | — | 35.4 | 28.7 | 68.2 | 2.1 | (Prasood e |
| 8 | Netravati-Gurpur Basin, Karnataka | 88.4 | 14.3 | 26.5 | 31.2 | 78.4 | 44.1 | 92.5 | — | (Vandana |
| 9 | Periyar River Basin, Kerala | — | 34.6 | 41.2 | 18.9 | 112.5 | 85.3 | 245.1 | 5.8 | (Kiruba et |
| 10 | Noyyal River Basin, Tamil Nadu | — | 42.1 | 56.4 | 22.8 | 312.4 | 189.5 | 294.2 | 8.4 | (P, 2024) |
| 11 | Bharathapuzha River Basin, Kerala | — | 12.4 | 21.1 | 14.5 | 72.8 | 8.1 | 15.3 | — | (Mathew 2022) |

*Note: "—" indicates elements that were not analyzed in that specific publication*

Table 6. Production and Cultivated area trends of major crops in the Kuppam River Basin (Source: Agricultural Statistics,2026).

| Crop | Cultivated area (ha) 2010 | Cultivated area (ha) 2024 | Trend | Production 2010 (t)* | Production 2024 (t)* | Trend |
|---|---|---|---|---|---|---|
| Paddy | 1448.94 | 585.45 | ↓↓↓ | 2692.72 | ND | — |
| Sugarcane | 0.29 | 0.08 | ↓ | ND | 10.05 | — |
| Pepper | 1345.2 | 628.95 | ↓↓ | 458.25 | 193.72 | ↓↓ |
| Ginger | 5.41 | 5.18 | → | 24.25 | 23.32 | → |
| Turmeric | 7.13 | 12.26 | ↑ | 21.03 | 60.49 | ↑↑ |
| Arecanut | 3260.4 | 2738.51 | ↓ | 4831.74 | 2281.18 | ↓↓ |
| Nutmeg | 88.79 | 73.44 | ↓ | 98.47 | 34.59 | ↓↓ |
| Jack† | 1086.72 | 1115.05 | ↑ | 3.8 | 3.31 | → |
| Banana | 92.74 | 46.9 | ↓↓ | 788.96 | 310.74 | ↓↓ |
| Plantain | 389.52 | 353.58 | ↓ | 1867.75 | 1702.13 | ↓ |
| Pineapple | 46.58 | 18.61 | ↓↓↓ | 179.01 | 168.68 | ↓ |
| Papaya | 258.63 | 225 | ↓ | 3197.18 | ND | — |
| Cashew | 3075.83 | 2647.53 | ↓ | 3403.17 | 1268.17 | ↓↓↓ |
| Tapioca | 291.79 | 180.68 | ↓↓ | 10365.26 | 6644.51 | ↓↓ |
| Drumstick | 189.44 | 236.78 | ↑ | 179.59 | ND | — |
| Coconut† | 10574.29 | 10438.61 | → | 79.28 | 67 | ↓ |
| Betel leaves | 2.71 | 1.53 | ↓ | 143.63 | 70.65 | ↓ |
| Cocoa | 111.55 | 96.6 | ↓ | 76.67 | 95.15 | ↑ |

Note -; ND- Data not available, ↑ Increase, ↓ Decrease, → Approximately stable, † Jack and coconut production are reported in **million numbers**, not tonnes.

Table 7 Fertilizer Consumption in Kannur (Source: Agricultural Statistics 2026)

| Fertilizer | Chemical Formula & Nutrients | 2021–22 | 2022–23 | 2023–24 | 2024–25 | 2025–26 | 5-Yr Average |
|---|---|---|---|---|---|---|---|
| UREA (Urea) | $CO(NH_2)_2$ • 46% Nitrogen (N) | 7139.43 | 5927.23 | 7485.35 | 6075.93 | 6594.09 | 6644.41 |
| MOP (Muriate of Potash) | KCl (Potassium Chloride) • 60% Potassium ($K_2O$) | 4645.60 | 4687.90 | 6797.53 | 5684.59 | 6816.60 | 5726.44 |

| | | | | | | | |
|---|---|---|---|---|---|---|---|
| FACTOMPHOS (Ammonium Phosphate Sulphate) | 40% AP + 60% AS • 20% N, 20% P, 13% S | 2984.75 | 2128.50 | 2900.57 | 2464.30 | 2622.60 | 2620.14 |
| DAP (Di-ammonium Phosphate) | $(NH_4)_2HPO_4$ • 18% N, 46% Phosphorus ($P_2O_5$) | 1716.10 | 1642.75 | 2096.38 | 1631.18 | 2811.65 | 1979.61 |
| SSP (Single Super Phosphate) | $Ca(H_2PO_4)_2$ + $CaSO_4$ • 16% P, 11% S, 19% Calcium | 580.00 | 433.85 | 504.05 | 290.44 | 423.55 | 446.38 |
| AS (Ammonium Sulphate) | $(NH_4)_2SO_4$ • 20.6% N, 23% Sulfur (S) | 42.25 | 29.50 | 51.95 | 39.00 | 32.00 | 38.94 |

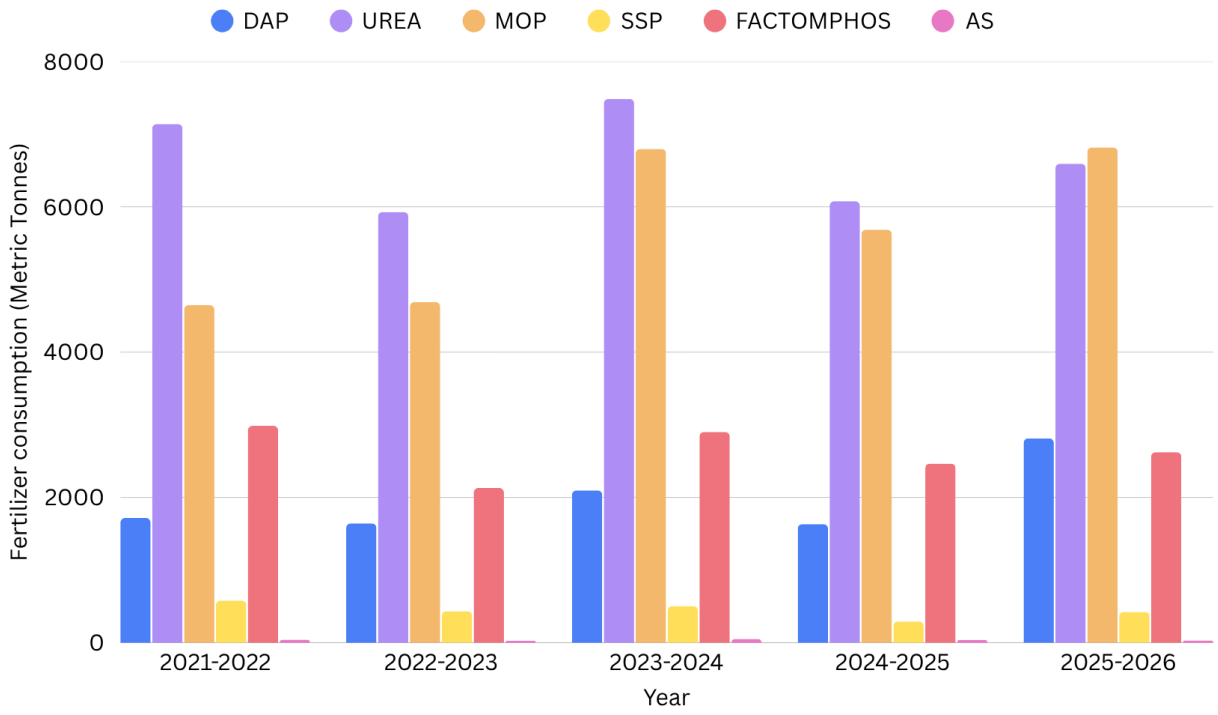



Fig.6 Fertilizer consumption trends in Kannur District, Kerala (2021–2026).

Table 8. Chemical pesticides consumption in metric tonne. (Source; Agricultural statistics 2026)

| YEAR | INSECTICIDES | FUNGICIDES | WEEDICIDES | RODENTICIDES AND FUMIGANTS | PLANT GROWTH REGULATORS | TOTAL |
|---|---|---|---|---|---|---|
| 2025-26 | 304.41 | 148.93 | 60.85 | 7.46 | 4.85 | 526.50 |
| 2024-25 | 302.04 | 159.15 | 80.97 | 7.78 | 16.28 | 566.22 |
| 2023-24 | 340.58 | 202.66 | 84.20 | 7.75 | 7.87 | 643.06 |
| 2022-23 | 310.05 | 121.98 | 92.62 | 6.91 | 8.30 | 539.86 |
| 2021-22 | 290.16 | 166.69 | 44.80 | 7.99 | 22.09 | 531.72 |

### 3.4 Pollution Assessment

The geoaccumulation index (Igeo) and the contamination factor (CF) were used to assess the level of potentially toxic element (PTE) contamination in the soils of the Kuppam River Basin, while the degree of contamination (Cd) and the pollution load index (PLI) were applied in order to evaluate the overall level of contamination (see **Tables 9 and 10**). Similar patterns were generally observed in both seasons, with slightly more enrichment during the non-monsoon season.

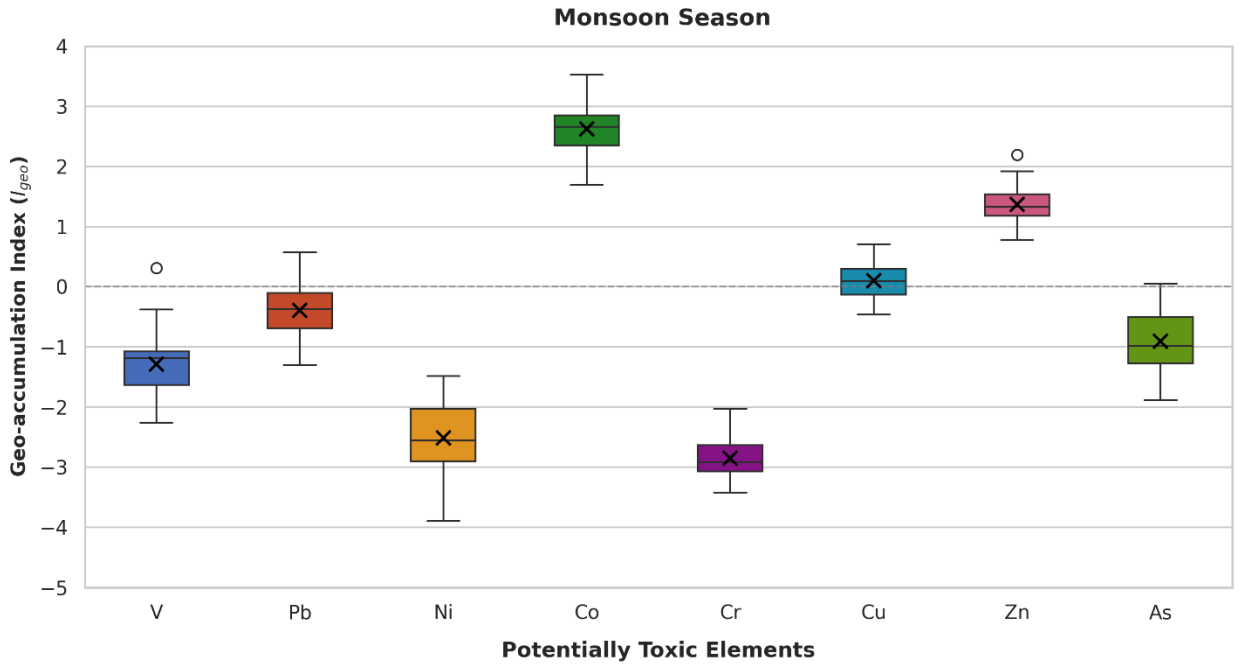
The Igeo values followed the order Co (2.60/2.54) > Zn (1.65/1.56) > Cu (0.61/0.47) > As (0.45/0.51) > Pb (−0.15/−0.39) > V (−1.36/−1.42) > Ni (−2.14/−2.15) > Cr (−3.92/−3.90) (non-monsoon/monsoon).Co showed the highest enrichment, indicating moderate-to-heavy contamination, followed by Zn with moderate contamination, whereas Cu showed comparatively low enrichment. **Fig. 7** shows the distribution of Igeo values for both seasons as box plots. Regional background values provide an important basis for distinguishing natural geochemical variability from potential anthropogenic enrichment(Kowalska et al., 2018). The CF analysis showed the same pattern (**Fig. 8**): Co had the highest contamination (9.88 and 9.36), followed by Zn, which showed considerable contamination (4.89 and 4.67). Cu, As, and Pb showed moderate contamination, with CF values of 2.47–2.21, 2.33–2.35, and 1.38–1.39, respectively. V, Ni, and Cr had CF values below 1, indicating a low level of contamination. The discrepancies between the CF and Igeo classifications, particularly for As, Pb, and Cu, are because different background corrections were used for these indices (Muller, 1969). The enrichment of Co is likely associated with lithogenic sources and weathering of Co-bearing minerals, potentially aided by its association with Fe–Mn oxides(Rodríguez-Trejo et al., 2026). The relatively higher Zn and Cu values may reflect combined lithogenic and possible agricultural inputs, including fertilizers, organic amendments, and crop-protective substances (Angon et al., 2024; Kakutey et al., 2023).In contrast, the negative Igeo values of Pb, As, V, Ni, and Cr indicate little or no enrichment relative to the selected regional background values, suggesting predominantly natural geochemical controls. During the non-monsoon period, the level of contamination (Cd) was 22.06, and during the monsoon period it was 21.08, indicating that there had been very high levels of contamination mainly caused by Co and Zn. The PLI values are 1.35 and 1.32 for non-monsoon and monsoon (**Fig. 9**), respectively, exceeding 1 and indicating overall pollution, with slightly higher enrichment during the non-monsoon season.To understand the pollution levels in the Kuppam River Basin, its data were compared with other river basins in India and around the world (**Table 11**)

Table 9. Geoaccumulation Index ($I_{geo}$) and Contamination Factor ($C_f$) for Kuppam soil during Non-Monsoon and Monsoon seasons.

| PTEs | Bn Value Used in the study | Igeo | | | Cf | | |
|---|---|---|---|---|---|---|---|
| | | Nonmonsoon | Monsoon | Category | Nonmonsoon | Monsoon | Category |
| **V** | 170 | -1.36 | -1.42 | Uncontaminated | 0.64 | 0.61 | Low contamination |
| **Pb** | 17 | -0.15 | -0.39 | Uncontaminated | 1.38 | 1.39 | Moderate contamination |
| **Ni** | 55.43 | -2.14 | -2.15 | Uncontaminated | 0.34 | 0.35 | Low contamination |
| **Co** | 17.3 | 2.60 | 2.54 | Moderately to heavily contaminated | 9.88 | 9.36 | Very high contamination |
| **Cr** | 171.86 | -3.92 | -3.90 | Uncontaminated | 0.13 | 0.13 | Low contamination |
| **Cu** | 37.14 | 0.61 | 0.47 | Uncontaminated to moderately polluted | 2.47 | 2.21 | Moderate contamination |
| **Zn** | 75.14 | 1.65 | 1.56 | Moderately contaminated | 4.89 | 4.67 | Considerable contamination |
| **As** | 4.8 | 0.45 | 0.51 | Uncontaminated to moderately contaminated | 2.33 | 2.35 | Moderate contamination |

Table 10. Seasonal Variation of Pollution Load Index (PLI).

| Season | Pollution Load Index (PLI) | Pollution Category |
|---|---|---|
| **Non-monsoon** | 1.35 | Polluted/Moderately polluted |
| **Monsoon** | 1.32 | Polluted/Moderately polluted |




(a)

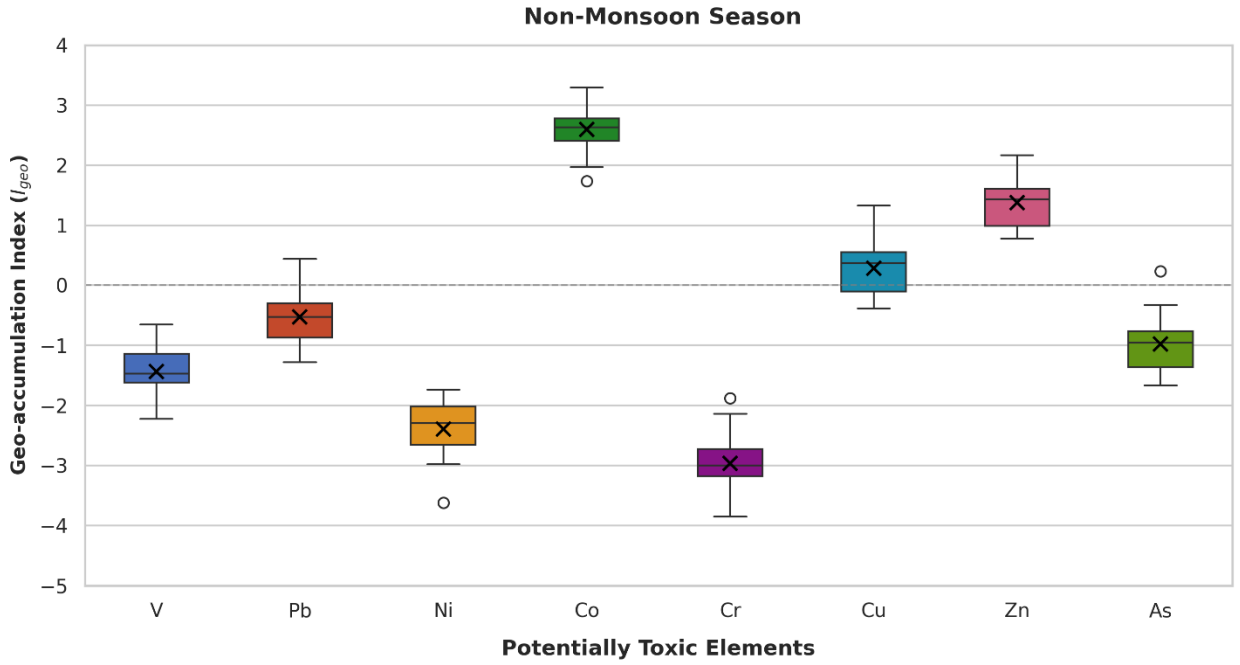



Fig 7 Seasonal distribution of Geo-accumulation Index ($I_{geo}$) values for Potentially Toxic Elements **(a)** Non-Monsoon Season and **(b)** Monsoon Season.

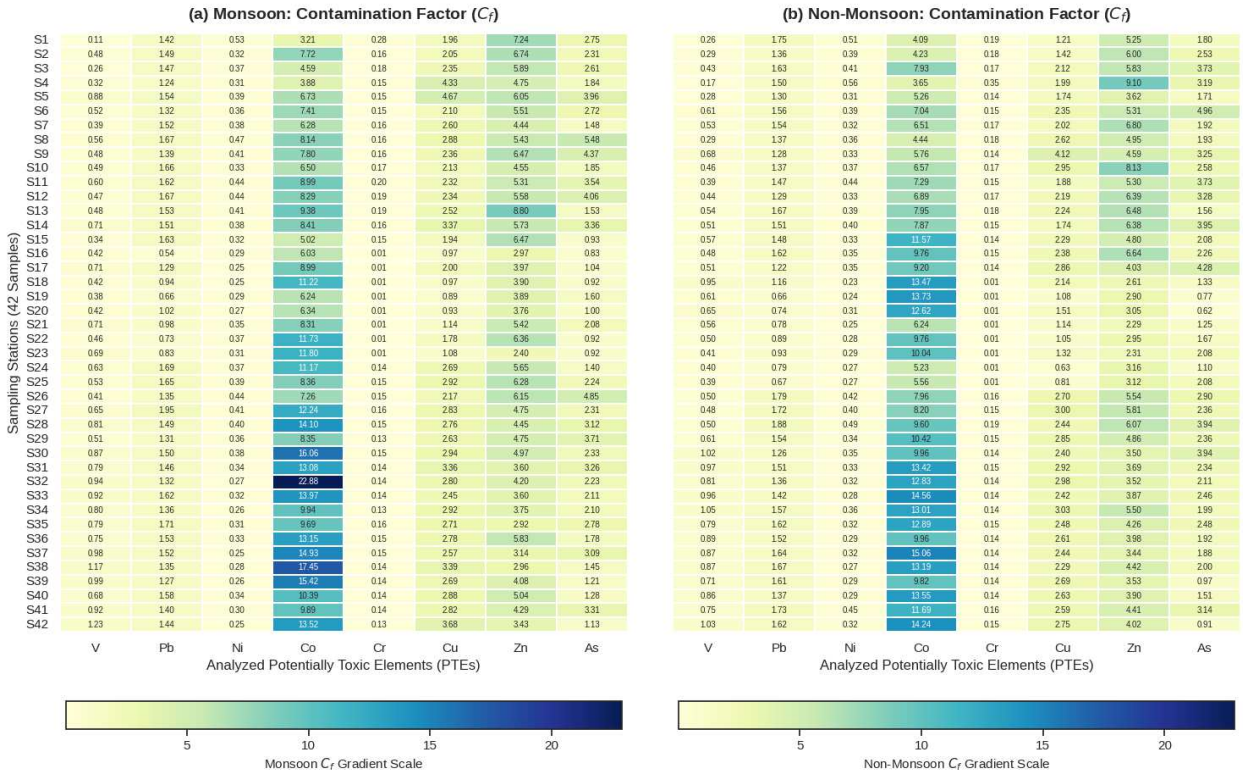



Fig 8. Contamination factor of potentially toxic elements across sampling locations during monsoon and non-monsoon seasons.

Table 11 Comparison of soil contamination metrics and pollution indices across various river basins.

| **No.** | River Basin & Country | **Elements Studied** | **Element-Specific Geo-accumulation Index (I_geo)** | **Element-Specific Contamination Factor (CF)** | **Pollution Load Index (PLI)** | **Reference** |
|---|---|---|---|---|---|---|
| **1** | Kuppam(Kerala, India) (average of both season) | V, Pb, Ni, Co, Cr, Cu, Zn, As | V: -1.39, Pb: -0.27, Ni: -2.14, Co: 2.57, Cr: -3.91, Cu: 0.54, Zn: 1.60, As: 0.48 | V: 0.63, Pb: 1.39, Ni: 0.35, Co: 9.62, Cr: 0.13, Cu: 2.34, Zn: 4.78, As: 2.34 | **1.33***(Polluted)* | *Current Study* |
| **2** | Periyar(Kerala, India) | V, Cr, Ni, Cu, Zn, Pb, As | NR | V: 1.10, Ni: 1.40, Cr: 1.25, Cu: 2.10, Zn: 2.80 | **1.45** | (Krishnakumar et al., 2022) |
| **3** | Karuvannur(Kerala, India) | V, Cr, Ni, Cu, Zn, Ga, Rb, | V: 0.05, Cr: -0.07, Ni: -0.98, Cu: -0.36, Zn: -0.79, Ga: - | V: 1.62, Cr: 1.54, Ni: 0.81, Cu: 1.26, Zn: 0.92, Ga: 1.47, Rb: 0.30, Sr: | **1.11** *(Moderately polluted)* | (Siji et al., 2025) |

| | | | | | | |
|---|---|---|---|---|---|---|
| | | Sr, Y, Zr, Ba, La | 0.06, Rb: -2.43, Sr: -0.98, Y: -1.13, Zr: 0.11, Ba: -0.88, La: -0.94 | 0.88, Y: 0.69, Zr: 1.85, Ba: 0.83, La: 0.83 | | |
| **4** | Yamuna (Delhi/NCR, India) | Pb, Zn, Ni, Cr, Cu, Cd | Pb: 1.14, Zn: 1.52, Cr: 0.24, Ni: 0.18 | Pb: 2.85, Zn: 3.42, Cr: 1.64, Ni: 1.38, Cu: 2.15, Cd: 4.22 | **2.21** *(Urban farm soil overprints)* | (Rajan & Nandimandalam, 2024) |
| **5** | Long An (Mekong, Vietnam) | Cu, Ni, Pb, Zn, Cd | Cu: 0.12, Ni: 0.35, Pb: -0.58 | Cu: 2.15, Ni: 2.40, Pb: 1.05, Zn: 1.32 | **1.64** *(Impacted by agrochemical loading)* | (Hoang et al., 2025) |
| **6** | Aries(Central Romania) | Cu, Ni, Zn, Pb, As, Cd | Pb: 0.45, Cu: 1.12, As: 0.88, Cd: 2.34 | Cu: 2.45, Pb: 1.88, As: 2.62, Cd: 5.12 | **2.24** *(Mining tailing outwash soils)* | (Moldovan et al., 2022) |
| **7** | Pra (South-Central Ghana) | As, Pb, Cd, Zn, Cr, Ni, Fe | As: -1.25, Pb: 0.84, Cd: 0.45, Cr: 0.32 | As: 0.65, Pb: 3.42, Cd: 4.88, Zn: 1.22, Cr: 2.15, Ni: 1.68 | **1.42** *(Unregulated illegal mining outwash)* | (Duncan et al., 2018) |
| **8** | Sematan-Serayan (Bengal Basin, India) | As, Pb, Cr, Cu, Zn, Ni | As: 0.15, Pb: -0.32, Cr: -0.48, Cu: -0.22 | As: 1.38, Pb: 1.15, Cr: 1.02, Cu: 1.28, Zn: 1.45, Ni: 1.10 | **1.24** *(Moderate domestic overprints)* | (Idrus & Ding, 2026) |
| **9** | Ruaha (Hunan, China) | Pb, Cd, Zn, Cu, As, Cr | Pb: 0.58, Cd: 1.94, As: 0.32, Cr: -0.12 | Pb: 2.34, Cd: 4.12, Zn: 1.65, Cu: 1.88, As: 1.54, Cr: 1.18 | **1.72** *(Industrial runoff accumulation)* | (Mng'ong'o, 2026) |
| **10** | Yellow River Delta (Shandong, China) | Cr, Ni, Cu, Zn, Pb, As, Cd | Cr: -0.14, Ni: -0.22, Pb: -0.35, As: 0.08 | Cr: 1.12, Ni: 1.20, Pb: 1.15, Cu: 1.24, Zn: 1.08, As: 1.54 | **1.21** *(Mainly geogenic loess background)* | (Miao et al., 2020; Zou et al., 2026) |

Note NR= Not Reported

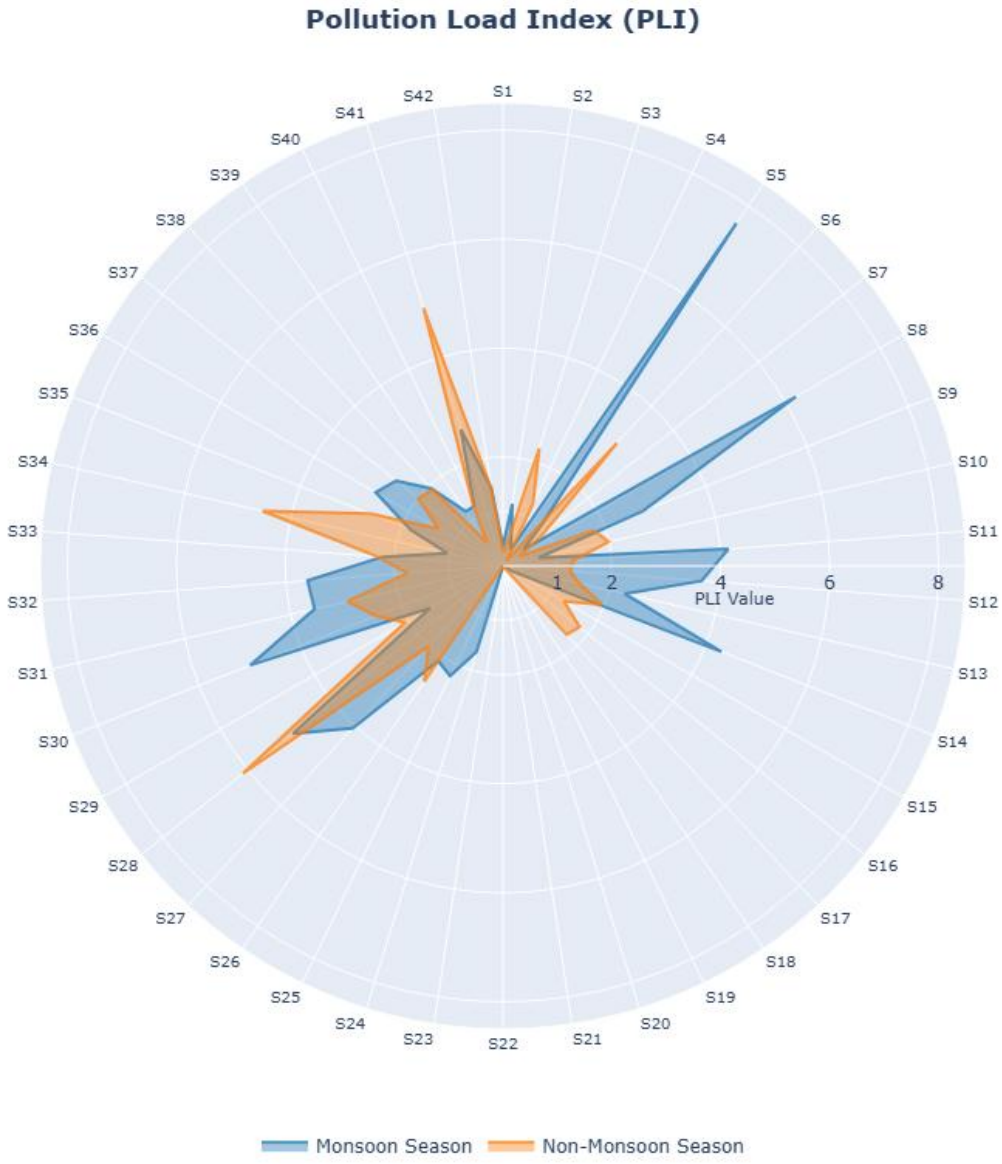



Fig 9. Radar plot of KRB soil for monsoon and non monsoon seasons.

### 3.5 Human Health Risk Assessment

#### 3.5.1 Non-carcinogenic Health Risk

**The** potential non-carcinogenic risks resulting from exposure to PTE via ingestion, dermal contact, and inhalation were evaluated for both adults and children (**Table 12**). Ingestion was **the** main route of exposure, followed by dermal contact, while inhalation played a relatively minor role, as earlier soil risk assessments found(Gupta et al., 2024; USEPA, 2011).

During the non-monsoon period, the adult Hazard Index (HI) values were 0.0892 for V, 0.0111 for Cr, 0.0572 for As, 0.0015 for Ni, 0.0260 for Pb, 0.0036 for Cu, and 0.0020 for Zn. For children, non-monsoon HI values were 0.1791

for V, 0.0752 for Cr, 0.3741 for As, 0.0096 for Ni, 0.1688 for Pb, 0.0230 for Cu, and 0.0124 for Zn; except for Cobalt, these elements remained safely below the threshold of 1. During the monsoon season, the adult HI values were 0.0799 for V, 0.0100 for Cr, 0.0523 for As, 0.0013 for Ni, 0.0229 for Pb, 0.0031 for Cu, and 0.0017 for Zn. Among children in the monsoon season, the HI values were 0.1633 for V, 0.0697 for Cr, 0.3360 for As, 0.0085 for Ni, 0.1498 for Pb, 0.0204 for Cu, and 0.0109 for Zn. While most studied elements remained below the safety threshold of 1.0, Cobalt (Co) represents a significant chronic non-carcinogenic health concern for children, exhibiting a child Hazard Index (HI) of 5.7002 in the non-monsoon season and 5.4024 in the monsoon season, thereby breaching the safe regulatory baseline limit under the assumed exposure conditions(USEPA, 1989, 2011).

The higher HI values for children indicate greater exposure when adjusted for body weight and age-specific soil-ingestion behavior. Cobalt was the primary non-carcinogenic concern for children because of its high ingestion hazard quotient, whereas arsenic was the leading non-carcinogenic concern among the other evaluated elements, showing that risk depends on the combined influence of concentration, exposure dose, and toxicity. The fact that arsenic had a high HI of 0.3741 in children during the non-monsoon season is also significant since chronic arsenic exposure is linked to systemic toxicity and carcinogenic effects(ATSDR, 2005, 2012, 2020, 2024b, 2024a). Unlike studies where lead is excluded due to model constraints, Pb was successfully evaluated here via ingestion, revealing low screening values (HI ≤ 0.1688) that do not, however, imply an absence of potential developmental health effects.

### 3.5.2 Carcinogenic Health Risk

Lifetime cancer risks (LCRs) were evaluated for arsenic (As) and nickel (Ni) using the applicable exposure pathways, while lead (Pb) risk was assessed through ingestion only using the USEPA risk-assessment framework (USEPA, 1989, 2011, 2026) (**Table 13**).Dermal carcinogenic risk for Lead was omitted due to the element's extremely poor dermal permeability factor (ABS_d ≤ 0.001) and the subsequent absence of a verified Dermal Cancer Slope Factor (SF_derm) in the USEPA RSL database, in accordance with USEPA RAGS Part E guidance. Similarly, inhalation cancer risks were excluded due to the absence of an EPA-sanctioned Inhalation Slope Factor (SF_inh), as the mass dose derived from soil-to-air particulate emission factors (PEF) represents a negligible systemic contribution to lifetime lung carcinogenicity compared to direct gastrointestinal absorption pathways.Chromium was excluded because WD-XRF cannot distinguish between Cr(III) and Cr(VI), Cr cancer-risk estimates are excluded.

Arsenic was the principal modeled carcinogenic-risk concern, with total LCRs exceeding the $10^{-4}$ upper screening benchmark for adults and children in both seasons. Non-monsoon LCRs were $2.20 \times 10^{-4}$ for adults and $3.07 \times 10^{-4}$ for children, decreasing to $1.99 \times 10^{-4}$ and $2.75 \times 10^{-4}$, respectively, during the monsoon. Ingestion dominated the estimated As risk, whereas dermal contributions were substantially lower and inhalation contributions were negligible ($\leq 10^{-12}$). Nickel LCRs remained within the $10^{-6}$ to $10^{-4}$ screening range, decreasing from $3.50 \times 10^{-5}$ in adults and $2.90 \times 10^{-5}$ in children during the non-monsoon season to $3.04 \times 10^{-5}$ and $2.52 \times 10^{-5}$, respectively, during the monsoon. Both ingestion and dermal contact contributed to the estimated Ni risks, while inhalation contributions were negligible ($\leq 10^{-10}$). Lead (Pb) ingestion-related LCRs remained below $10^{-6}$ for both adults and children across seasons. These estimates represent screening-level risks under the selected exposure assumptions and should not be interpreted as predictions of actual health outcomes.

The results identify As as the principal modeled carcinogenic-risk concern, particularly for children, consistent with their greater exposure relative to body weight under the adopted USEPA assumptions (USEPA, 1989, 2011).The spatial heterogeneity of carcinogenic risks in the basin shows a clear overlap between high risk zones and the regional history of agricultural management. The Extreme Hotspots are closely aligned with sectors showing long-term soil retention of legacy arsenical compounds traditionally found in historical weedicides, insecticides and fungicides. Elevated Toxicity Points, meanwhile, show a more widespread non-point source signature. The pattern is largely the result of long term repeated applications of phosphate fertilisers(Mandal & Suzuki, 2002; Nziguheba & Smolders, 2008).The pristine trends observed in Safe / Tolerable Zones (Samples 15–18 and 20–23) are ambient baseline conditions away from intensive farming, and provide an ideal environmental control for basin mapping.The hotspot zoning of carcinogenic human health risks across the basin, along with their primary geogenic and agricultural drivers, are summarized in **Table 14**

The temporal variation in reported cancer cases in the study area (**Fig. 10; Table S7**) provides local health context. **Table S8** summarizes the major toxicological effects of selected PTEs. Comparison with risk assessments from other Indian and international river basins (**Table 15**) further contextualizes the Kuppam findings.

517 Table 12. Seasonal Non-Carcinogenic assessment in the basin.

| Season | Element | Receptor | Ingestion (HQ_ing) | Dermal (HQ_derm) | Inhalation (HQ_inh) | Hazard Index (HI) |
|---|---|---|---|---|---|---|
| **Non-Monsoon** *(42-Site Summary)* | V | Adults | 0.0221 | 0.0672 | $2.08 \times 10^{-6}$ | 0.0892 |
| | | Children | 0.1544 | 0.0247 | $4.33 \times 10^{-6}$ | 0.1791 |
| | Pb | Adults | 0.0240 | 0.0020 | $8.99 \times 10^{-7}$ | 0.0260 |
| | | Children | 0.1681 | 0.0007 | $1.89 \times 10^{-6}$ | 0.1688 |
| | Ni | Adults | 0.0014 | 0.0002 | $1.25 \times 10^{-7}$ | 0.0015 |
| | | Children | 0.0096 | 0.0001 | $2.61 \times 10^{-7}$ | 0.0096 |
| | Co | Adults | 0.8137 | 0.0041 | $2.15 \times 10^{-3}$ | 0.8199 |
| | | Children | 5.6960 | 0.0011 | $3.11 \times 10^{-3}$ | **5.7002** |
| | Cr | Adults | 0.0107 | 0.0003 | $1.05 \times 10^{-4}$ | 0.0111 |
| | | Children | 0.0746 | 0.0004 | $2.19 \times 10^{-4}$ | 0.0752 |
| | Cu | Adults | 0.0033 | 0.0003 | $3.08 \times 10^{-7}$ | 0.0036 |
| | | Children | 0.0229 | 0.0001 | $6.43 \times 10^{-7}$ | 0.0230 |
| | Zn | Adults | 0.0018 | 0.0003 | $1.65 \times 10^{-7}$ | 0.0020 |
| | | Children | 0.0123 | 0.0001 | $3.44 \times 10^{-7}$ | 0.0124 |
| | As | Adults | 0.0532 | 0.0040 | $1.22 \times 10^{-5}$ | 0.0572 |
| | | Children | 0.3726 | 0.0015 | $2.55 \times 10^{-5}$ | 0.3741 |
| **Monsoon** *(42-Site Summary)* | V | Adults | 0.0198 | 0.0601 | $1.94 \times 10^{-6}$ | 0.0799 |
| | | Children | 0.1412 | 0.0221 | $3.98 \times 10^{-6}$ | 0.1633 |
| | Pb | Adults | 0.0211 | 0.0018 | $8.11 \times 10^{-7}$ | 0.0229 |
| | | Children | 0.1492 | 0.0006 | $1.66 \times 10^{-6}$ | 0.1498 |
| | Ni | Adults | 0.0012 | 0.0001 | $1.12 \times 10^{-7}$ | 0.0013 |
| | | Children | 0.0084 | 0.0001 | $2.35 \times 10^{-7}$ | 0.0085 |
| | Co | Adults | 0.7712 | 0.0039 | $2.04 \times 10^{-3}$ | 0.7751 |
| | | Children | 5.3984 | 0.0010 | $2.95 \times 10^{-3}$ | **5.4024** |
| | Cr | Adults | 0.0098 | 0.0002 | $9.85 \times 10^{-5}$ | 0.0100 |
| | | Children | 0.0694 | 0.0003 | $1.95 \times 10^{-4}$ | 0.0697 |
| | Cu | Adults | 0.0029 | 0.0002 | $2.65 \times 10^{-7}$ | 0.0031 |

| | | | | | | |
|---|---|---|---|---|---|---|
| | | Children | 0.0203 | 0.0001 | $5.48 \times 10^{-7}$ | 0.0204 |
| | Zn | Adults | 0.0015 | 0.0002 | $1.42 \times 10^{-7}$ | 0.0017 |
| | | Children | 0.0108 | 0.0001 | $2.99 \times 10^{-7}$ | 0.0109 |
| | As | Adults | 0.0487 | 0.0036 | $1.10 \times 10^{-5}$ | 0.0523 |
| | | Children | 0.3348 | 0.0012 | $2.24 \times 10^{-5}$ | 0.3360 |

Table 13. Cancer risk Associated with exposure to potentially toxic elements in soils through ingestion and dermal pathways

| **Season** | **Element** | **Receptor** | **Ingestion Risk** | **Dermal Risk** | **Inhalation Risk** | **Total Lifetime Cancer Risk (LCR)** |
|---|---|---|---|---|---|---|
| **Non-Monsoon** (42-Site Mean Summary) | As | Adults | $2.19 \times 10^{-4}$ | $7.63 \times 10^{-7}$ | $2.77 \times 10^{-12}$ | **$2.20 \times 10^{-4}$** |
| | | Children | $3.07 \times 10^{-4}$ | $5.61 \times 10^{-8}$ | $1.16 \times 10^{-12}$ | **$3.07 \times 10^{-4}$** |
| | Ni | Adults | $1.99 \times 10^{-5}$ | $1.51 \times 10^{-5}$ | $9.25 \times 10^{-10}$ | $3.50 \times 10^{-5}$ |
| | | Children | $2.79 \times 10^{-5}$ | $1.11 \times 10^{-6}$ | $3.86 \times 10^{-10}$ | $2.90 \times 10^{-5}$ |
| | Pb | Adults | $1.22 \times 10^{-7}$ | / | / | $1.22 \times 10^{-7}$ |
| | | Children | $1.71 \times 10^{-7}$ | / | / | $1.71 \times 10^{-7}$ |
| **Monsoon** (42-Site Mean Summary) | As | Adults | $1.98 \times 10^{-4}$ | $6.82 \times 10^{-7}$ | $2.41 \times 10^{-12}$ | **$1.99 \times 10^{-4}$** |
| | | Children | $2.75 \times 10^{-4}$ | $4.91 \times 10^{-8}$ | $1.01 \times 10^{-12}$ | **$2.75 \times 10^{-4}$** |
| | Ni | Adults | $1.74 \times 10^{-5}$ | $1.30 \times 10^{-5}$ | $8.21 \times 10^{-10}$ | $3.04 \times 10^{-5}$ |
| | | Children | $2.42 \times 10^{-5}$ | $9.62 \times 10^{-7}$ | $3.37 \times 10^{-10}$ | $2.52 \times 10^{-5}$ |
| | Pb | Adults | $1.08 \times 10^{-7}$ | / | / | $1.08 \times 10^{-7}$ |
| | | Children | $1.50 \times 10^{-7}$ | / | / | $1.50 \times 10^{-7}$ |

Table 14 Carcinogenic risk zoning and environmental drivers for sampling locations.

| Risk Classification Zone | TCR Threshold Range | Specific Sample Location Numbers | Primary Hypothesized Geochemical & Environmental Influences |
|---|---|---|---|
| **Extreme Hotspots** | LCR ≥ $3.0 \times 10^{-4}$ | **5, 8, 9, 11, 12, 14, 26, 29, 31, 41** | Intensive point-source inputs; historic accumulation of persistent agrochemicals (insecticides, weedicides, fungicides); concentrated low-lying drainage deposition zones. |
| **Elevated Toxicity Points** | $1.1 \times 10^{-4}$ to $3.0 \times 10^{-4}$ | **1, 2, 3, 4, 6, 10, 19, 21, 25, 27, 28, 30, 32, 33, 34, 35, 36, 37, 40** | Continuous non-point source application of raw rock phosphate-derived fertilizers (DAP, SSP, FACTOMPHOS); baseline geogenic weathering of arsenic-bearing sulfide minerals. |
| **Borderline Exposure Risks** | $1.0 \times 10^{-4} \leq$ LCR $\leq 1.1 \times 10^{-4}$ | **7, 13, 24, 38, 39, 42** | Normal geogenic background variations combined with localized surface runoff and trace mineral deposition from synthetic potassium boosters (MOP). |
| **Safe / Tolerable Zones** | LCR < $1.0 \times 10^{-4}$ | **15, 16, 17, 18, 20, 22, 23** | Ambient baseline geogenic control sectors; pristine upstream catchment areas; absence of intensive chemical-based cultivation or industrial inputs. |

525

526 Table 15 Comparative human health risks from potentially toxic elements in river-basin soils.

| No. | River Basin & Country | Soil PTEs Assessed | Population Group | Total Cancer Risk (TCR) | Non-Carcinogenic Hazard Index (HI) | Reference Source |
|---|---|---|---|---|---|---|
| 1 | Kuppam River Basin (India) [Monsoon] | V, Ni, Co, Pb Cr, Cu, Zn, As | Adults<br>Children | $2.43 \times 10^{-4}$<br>$3.09 \times 10^{-4}$ | 0.95<br>6.16 | *Current Study* |
| 2 | Ganga River Basin (India) | Cd, As, Cr, Ga, Cu, Pb | Adults<br>Children | $2.10 \times 10^{-5}$<br>$1.13 \times 10^{-4}$ | 0.32<br>1.73 | (Kumar & Anshumali, 2025b) |
| 3 | Damodar River Basin (India) | Fe, Mn, Cu, Zn, B | Adults<br>Children | NR<br>NR | 0.015<br>0.084 | (Hoque et al., 2023b) |
| 4 | Dravyavati River Basin (India) | Pb, Ni, Cr, Cu, Zn | Adults<br>Children | NR<br>NR | 0.55<br>1.24 | (Mittal & Kaushik, 2026) |
| 5 | Yellow River Basin (China) | As, Cd, Cr, Cu, Hg, Ni, Pb, Zn | Adults<br>Children | NR<br>NR | 0.11<br>0.54 | (Li et al., 2024) |
| 6 | Yangtze River Basin (China) | Pb, Cd, As, Cr, Zn | Adults<br>Children | $1.40 \times 10^{-5}$<br>$4.80 \times 10^{-5}$ | 0.24<br>0.91 | (Mishra et al., 2025) |
| 7 | Wanchuan River Basin (China) | Ni, As, Zn, Cr, Cu | Adults<br>Children | NR<br>NR | 0.38<br>0.89 | (E. Yang et al., 2024) |

| | | | | | | |
|---|---|---|---|---|---|---|
| 8 | Heihe River Basin (China) | Cd, As, Zn, Cu, Ni, Cr | Adults<br>Children | $8.20 \times 10^{-6}$<br>$2.10 \times 10^{-5}$ | 0.09<br>0.41 | (Huang et al., 2025) |
| 9 | Hubei Catchment Basin (China) | Cr, Ni, Pb, As, Cd, Cu, Zn, Ba | Adults<br>Children | $5.75 \times 10^{-4}$<br>$9.44 \times 10^{-4}$ | 1.03<br>7.31 | (Gan et al., 2022) |
| 10 | Witwatersrand Basin (S. Africa) | Cr, Ni, As, Zn, Cu, Co, Pb, Hg, Cd | Adults<br>Children | $1.70 \times 10^{-1}$<br>$3.67 \times 10^{-1}$ | 2.13<br>43.80 | (Kamunda et al., 2016) |

Note NR= Not Reported

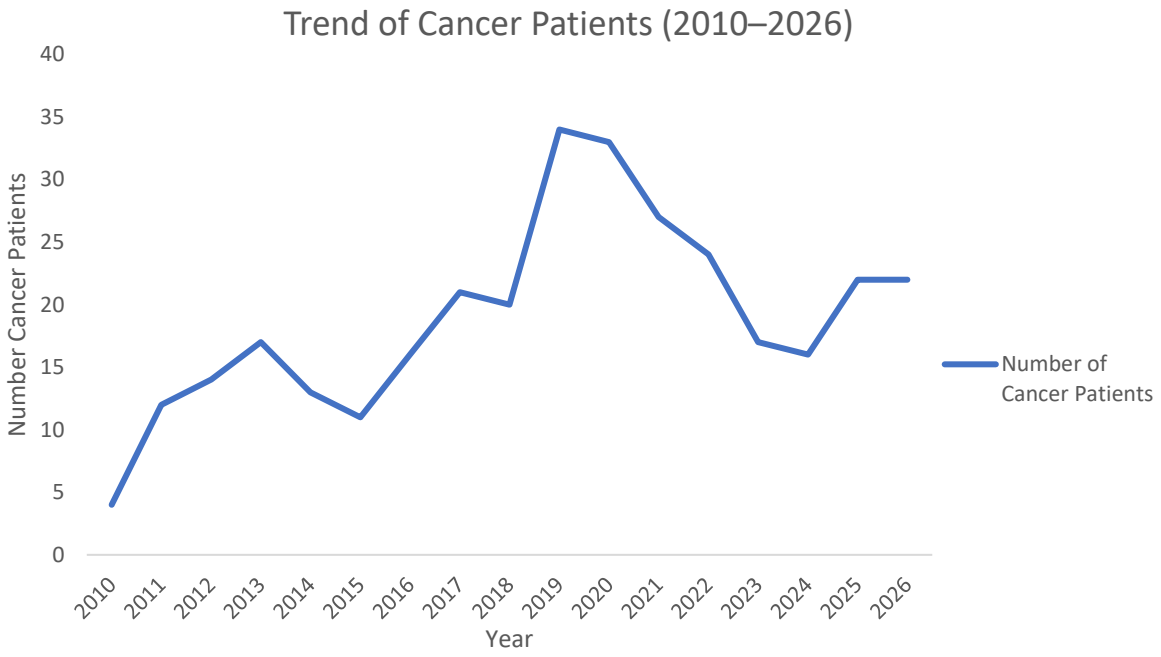



Fig. 10 Cancer case trend in KRB

### 3.6 A multivariate assessment of the associations between PTEs and source signatures

The elemental associations and possible source signatures in the soils of the KRB for the non-monsoon and monsoon seasons were assessed using a Pearson correlation analysis and Positive Matrix Factorization (PMF) ( **Fig. 11 and Fig. 12)**. While the Pearson correlation revealed significant relationships between the major and potentially toxic elements (PTEs), the PMF supplied multielement factor profiles. Taken together, these methods show the relative impact of lithogenic, pedogenic, agricultural, and local anthropogenic processes.

#### 3.6.1 Positive Matrix Factorization

In both seasons, PMF identified three factors, and the three-factor solution provided the most interpretable elemental profiles in relation to the basin's geological and land-use conditions (**Table 16**). A three-factor solution was selected based on PMF model diagnostics and factor interpretability, providing an optimal balance between model fit, residual structure, and environmentally meaningful source profiles without unnecessary factor splitting. Reported values of $Q_{robust}$ and $Q_{true}$ are 2264.13 and 2546.93, respectively. $Q_{truet}/Q_{exp}$ ratio is 4.421753. Seasonal variations in factor

contributions may indicate changes in weathering, leaching, erosion, and sediment redistribution (Mao et al., 2022; Paatero, 1997; Paatero & Tapper, 1993, 1994) .

In the non-monsoon period (non-monsoon season, Factor 1 was characterized by Mn (~85%), V (~73%), Co (~71%), Fe (~62%), Al (~48%), and Ti (~42%), which shows a mainly lithogenic–pedogenic origin. The fact that iron, aluminum, and titanium occur together with relatively immobile trace elements is in agreement with weathered parent material and secondary soil phases(Taylor & McLennan, 1985). Factor 2 consisted of Na (>90%), Ca (~75%), K (~44%), Mg (~34%), and P (~30%), reflecting a combination of weathering and agricultural influences. The association between sodium, calcium, potassium, and magnesium is in agreement with the weathering of primary silicate minerals and the release of base cations (Bland & Rolls, 2016).The presence of phosphorus indicates an extra agricultural influence. The amounts of phosphorus, along with sodium, calcium, potassium, and magnesium, are consistent with both mineral weathering and possible agricultural inputs. Recorded patterns of crop cultivation and fertilizer application rates in the Kuppam basin support this explanation by providing independent evidence of an agricultural contribution to this factor. Factor 3 was dominated by Cr (~87%), As (~64%), Pb (~51%), Cu (~50%), Zn (~47%), and Ni (~45%), showing a mixed natural and anthropogenic origin, with possible inputs from agricultural and local anthropogenic sources.

In the monsoon season, Factor 1 consisted of Mn (~62%), Fe (~39%), P (~35%), Ti (~33%), Al (~30%), and Mg (~24%), showing that the main controls were lithogenic and pedogenic in nature, with an agricultural influence. Factor 2, with Na (~57%), K (~42%), Cu (~42%), Zn (~35%), Ni (~31%), and Al (~29%), showed a combination of weathering and agricultural characteristics. Factor 3, which was dominated by Cr (~78%), Ca (~65%), As (~56%), Co (~44%), and V (~37%), revealed a mixed geogenic and anthropogenic signature with a strong natural element.

Overall, the evidence shows that lithogenic and pedogenic processes form the main geochemical background, with agricultural and local anthropogenic effects added on top. The consistency of various elemental associations across seasons supports common geochemical controls, while seasonal changes in factor composition point to redistribution and differential mobility.

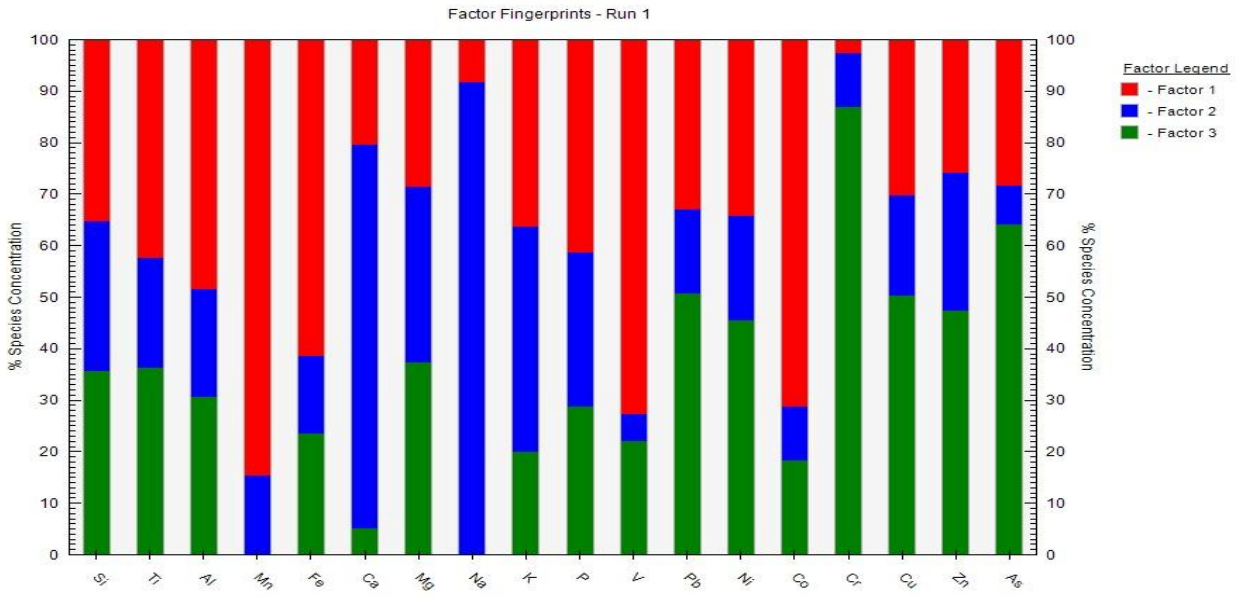



Fig 11. Source apportionment of potentially toxic elements during the non monsoon season.

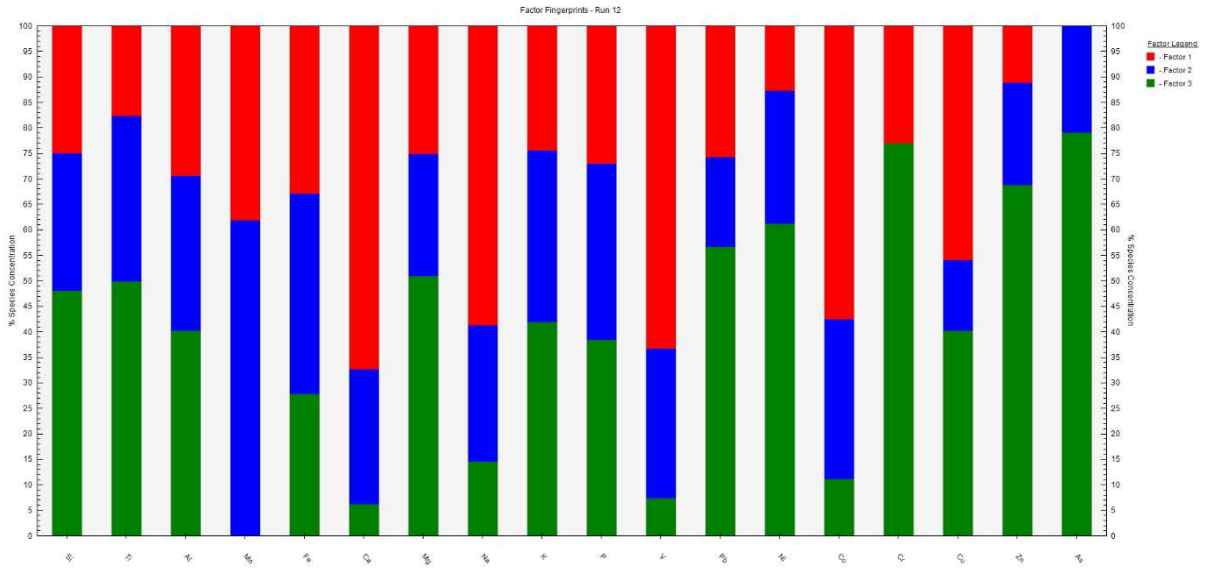



Fig 12**.** Source apportionment of potentially toxic elements during the monsoon season.

Table 16. Summary of PMF source factors and their interpreted sources for soils in the Kuppam River Basin.

| **Season** | **Factor** | **Dominant elements** | **Interpreted source** | **Supporting evidence** |
|---|---|---|---|---|
| Non-monsoon | F1 | Mn, Fe, V, Co, Al, Ti | Lithogenic | Charnockite, granitic gneiss, natural weathering |
| | F2 | Na, Ca, K, Mg, P | Weathering + Agricultural | Weathering products, fertilizer inputs |
| | F3 | Cr, As, Pb, Cu, Zn, Ni | Localized anthropogenic | Agriculture, road traffic, settlements |
| Monsoon | F1 | Mn, Fe, Ti, Al, Mg | Lithogenic | Parent rock weathering |
| | F2 | Na, K, Cu, Zn, Ni | Weathering + Agricultural | Nutrient inputs, cultivation |
| | F3 | Ca, Cr, As, Co, V | Mixed geogenic + anthropogenic | Weathering, agricultural activities |

### 3.6.2 Pearson Correlation Analysis

Seasonal Pearson correlation matrices (**Table 17 & Table 18**) showed persistent, season-dependent relationships between major-element oxides and PTEs.Al correlated positively with both Na and K, whereas Si correlated positively with Fe and Mn, suggesting associations between aluminosilicate and Fe–Mn-containing mineral phases. Associations between Al–Na/K and Si–Fe/Mn may indicate common mineralogical or geochemical controls, while relationships among Ca, Mg, and Na may suggest effects of mineral weathering and element redistribution(S. Yang et al., 2026).

The reported associations of V–Co, Pb–Cr, and Ni–Zn among the PTEs deserve consideration with their respective seasonal correlation coefficients. Seasonal differences were also apparent, as associations among Ca, Na, Cr, Pb, Zn, and Co were stronger during the monsoon, implying changes in element redistribution under increased hydrological activity(Pescke et al., 2026). In contrast, weaker or negative associations involving Fe and K, Mn and Cr, and V and K suggest different degrees of mobility and fractionation. These relationships show that mineralogical and weathering processes exert important controls, although correlation alone is not sufficient to distinguish between geogenic and anthropogenic sources.

Table 17. Pearson correlation analysis for Non-Monsoon

| | *Si* | *Ti* | *Al* | *Mn* | *Fe* | *Ca* | *Mg* | *Na* | *K* | *P* | *V* | *Pb* | *Ni* | *Co* | *Cr* | *Cu* | *Zn* | *As* |
|---|---|---|---|---|---|---|---|---|---|---|---|---|---|---|---|---|---|---|
| Si | 1.00 | | | | | | | | | | | | | | | | | |
| Ti | -0.20 | 1.00 | | | | | | | | | | | | | | | | |
| Al | -0.26 | -0.14 | 1.00 | | | | | | | | | | | | | | | |
| Mn | -0.57 | -0.12 | 0.07 | 1.00 | | | | | | | | | | | | | | |
| Fe | -0.70 | 0.41 | -0.10 | 0.53 | 1.00 | | | | | | | | | | | | | |
| Ca | 0.16 | -0.15 | -0.34 | -0.20 | -0.23 | 1.00 | | | | | | | | | | | | |
| Mg | 0.33 | 0.10 | -0.32 | -0.19 | -0.13 | 0.53 | 1.00 | | | | | | | | | | | |
| Na | 0.34 | -0.27 | -0.50 | -0.23 | -0.42 | 0.82 | 0.41 | 1.00 | | | | | | | | | | |
| K | 0.45 | -0.43 | -0.37 | -0.10 | -0.56 | 0.28 | 0.04 | 0.56 | 1.00 | | | | | | | | | |
| P | 0.08 | 0.03 | -0.40 | -0.05 | 0.06 | 0.20 | 0.25 | 0.31 | 0.19 | 1.00 | | | | | | | | |
| V | -0.07 | -0.38 | 0.26 | 0.56 | 0.15 | 0.02 | 0.03 | -0.07 | -0.18 | 0.01 | 1.00 | | | | | | | |
| Pb | 0.54 | 0.10 | 0.24 | -0.35 | -0.35 | -0.14 | 0.26 | -0.15 | -0.16 | 0.02 | 0.19 | 1.00 | | | | | | |
| Ni | 0.11 | 0.73 | -0.11 | -0.39 | 0.13 | -0.05 | 0.30 | -0.25 | -0.29 | 0.01 | -0.45 | 0.38 | 1.00 | | | | | |
| Co | -0.17 | -0.22 | 0.20 | 0.65 | 0.23 | -0.07 | 0.18 | -0.12 | -0.20 | -0.16 | 0.78 | 0.08 | -0.36 | 1.00 | | | | |
| Cr | 0.66 | 0.20 | -0.10 | -0.48 | -0.33 | 0.02 | 0.53 | -0.01 | -0.13 | 0.01 | -0.01 | 0.80 | 0.56 | -0.05 | 1.00 | | | |
| Cu | 0.56 | -0.15 | -0.13 | -0.21 | -0.23 | 0.34 | 0.44 | 0.19 | 0.02 | 0.24 | 0.46 | 0.59 | 0.11 | 0.22 | 0.57 | 1.00 | | |
| Zn | 0.34 | 0.50 | -0.20 | -0.55 | -0.15 | 0.06 | 0.29 | -0.07 | -0.05 | 0.09 | -0.50 | 0.29 | 0.67 | -0.39 | 0.44 | 0.09 | 1.00 | |
| As | 0.03 | 0.24 | 0.04 | -0.18 | 0.24 | 0.01 | 0.40 | -0.25 | -0.33 | 0.18 | -0.02 | 0.41 | 0.60 | -0.13 | 0.50 | 0.34 | 0.27 | 1.00 |

Table 18. Pearson correlation analysis for Monsoon

| | *Si* | *Ti* | *Al* | *Mn* | *Fe* | *Ca* | *Mg* | *Na* | *K* | *P* | *V* | *Pb* | *Ni* | *Co* | *Cr* | *Cu* | *Zn* | *As* |
|---|---|---|---|---|---|---|---|---|---|---|---|---|---|---|---|---|---|---|
| Si | 1.00 | | | | | | | | | | | | | | | | | |
| Ti | 0.12 | 1.00 | | | | | | | | | | | | | | | | |
| Al | -0.12 | -0.22 | 1.00 | | | | | | | | | | | | | | | |
| Mn | -0.63 | -0.08 | -0.17 | 1.00 | | | | | | | | | | | | | | |
| Fe | -0.49 | 0.29 | -0.28 | 0.46 | 1.00 | | | | | | | | | | | | | |
| Ca | 0.15 | -0.21 | -0.26 | -0.06 | -0.04 | 1.00 | | | | | | | | | | | | |
| Mg | 0.56 | 0.30 | -0.38 | -0.42 | -0.05 | 0.37 | 1.00 | | | | | | | | | | | |
| Na | 0.37 | -0.16 | -0.43 | -0.12 | -0.26 | 0.69 | 0.54 | 1.00 | | | | | | | | | | |
| K | 0.30 | -0.27 | 0.01 | -0.21 | -0.64 | 0.03 | 0.03 | 0.20 | 1.00 | | | | | | | | | |
| P | -0.14 | 0.03 | -0.21 | 0.36 | 0.17 | 0.29 | 0.03 | 0.03 | -0.08 | 1.00 | | | | | | | | |
| V | -0.20 | -0.14 | 0.39 | 0.35 | 0.39 | 0.09 | -0.21 | -0.15 | -0.44 | 0.07 | 1.00 | | | | | | | |
| Pb | 0.56 | 0.27 | 0.50 | -0.63 | -0.32 | -0.10 | 0.34 | -0.11 | 0.03 | -0.19 | 0.14 | 1.00 | | | | | | |
| Ni | 0.45 | 0.50 | 0.08 | -0.59 | -0.26 | -0.13 | 0.46 | -0.09 | 0.31 | -0.06 | -0.44 | 0.60 | 1.00 | | | | | |
| Co | -0.25 | -0.08 | 0.34 | 0.45 | 0.36 | -0.01 | -0.16 | -0.13 | -0.40 | -0.03 | 0.83 | 0.08 | -0.43 | 1.00 | | | | |
| Cr | 0.70 | 0.32 | 0.14 | -0.76 | -0.39 | 0.16 | 0.50 | 0.11 | 0.17 | -0.05 | -0.16 | 0.78 | 0.76 | -0.24 | 1.00 | | | |
| Cu | 0.40 | 0.17 | 0.09 | -0.26 | 0.12 | 0.35 | 0.45 | 0.13 | -0.33 | 0.30 | 0.46 | 0.59 | 0.16 | 0.28 | 0.49 | 1.00 | | |
| Zn | 0.51 | 0.42 | 0.03 | -0.62 | -0.31 | 0.00 | 0.32 | -0.08 | 0.09 | 0.05 | -0.41 | 0.56 | 0.73 | -0.45 | 0.79 | 0.26 | 1.00 | |
| As | 0.16 | 0.26 | -0.05 | -0.40 | 0.26 | 0.10 | 0.40 | -0.11 | -0.20 | 0.05 | -0.17 | 0.37 | 0.57 | -0.27 | 0.47 | 0.30 | 0.44 | 1.00 |

## 4. Conclusion

The study provides a preliminary geochemical baseline of the soils of the Kuppam River Basin (KRB) in the southern Western Ghats, India, through characterisation of potentially toxic elements (PTEs), seasonal comparison, positive matrix factorisation (PMF), and screening-level human-health risk assessment. Cobalt was the most enriched element relative to average crustal abundance, followed by zinc and copper, and most of the other elements were relatively less enriched. These patterns show the necessity of differentiating natural geochemical enrichment from possible anthropogenic inputs before interpreting soil contamination. The three-factor PMF model identified potential source signatures consistent with lithogenic and pedogenic processes, mineral weathering and possible agricultural and local anthropogenic influences. While the monsoon and non-monsoon geochemical patterns were largely comparable, seasonal differences highlight the need for repeated measurements to assess the temporal variability of PTE patterns. Screening level risk estimates identified cobalt as the principal contributor to the estimated non-carcinogenic risk and arsenic and nickel as contributors to the estimated carcinogenic risk. Children generally had higher estimated risks than adults because of differences in the exposure parameters used. These estimates depend on the selected exposure pathways and assumptions and represent potential risks that require further evaluation, not confirmed adverse health outcomes. Accordingly, the findings provide a basis for establishing baseline conditions, prioritising sites and elements for follow-up investigation, and guiding targeted monitoring across contrasting geological and land-use settings.

The broader scientific contribution lies in demonstrating a transferable catchment-scale framework that combines seasonal soil geochemistry, contamination indices, potential-source screening, and screening-level health-risk modelling. By linking these complementary lines of evidence, the approach provides a structured basis for comparing geochemical patterns and identifying priorities for further investigation in tropical catchments, including regions where environmental datasets remain limited. The framework can be applied to other river basins to improve the comparability of regional soil-geochemical assessments and thus support evidence-based environmental monitoring and resource management. Future studies should validate inferred source contributions with independent geological, land-use, and geochemical evidence; investigate the environmental mobility and bioavailability of priority elements; and improve health risk estimates with locally relevant exposure data. The study therefore contributes to SDG 15 by better understanding the soil geochemistry and to SDG 3 by preliminarily identifying potential concerns related to exposure, without directly showing ecosystem damage or soil-related disease. The KRB dataset and assessment framework provide a basis for focused follow-up studies and more informed catchment-scale soil management.

## Acknowledgment

The authors are very much thankful to the Director, NCESS, for providing research facilities, encouragement, and support. The authors greatly appreciate the financial support of MoES, Government of India (SAGE). One of the authors, Olin B. Jose, wishes to express her gratitude to Kannur University for granting a PhD research opportunity by providing the Junior Research Fellowship. The help rendered by the Directorate of Agriculture, Thiruvanthapuram is also gratefully acknowledged. The support provided by the Department of Forest and Wildlife, Government of Kerala, is duly acknowledged.

## Declaration of generative AI in scientific writing

This declaration confirms the use of generative AI tools in preparing this manuscript. In preparing this manuscript. the authors used ChatGPT and Grammarly to improve the language, grammar, and overall readability. The authors used generative AI tools, including but not limited to text generators, summarization tools, and language enhancers, to refine and structure the manuscript. These tools helped with grammar correction, sentence structuring, and minor language edits, ensuring clarity and precision in scientific communication.

## Declaration of competing interests

We declare no conflict of interest in the submission of this manuscript, and all authors approve it for publication. I declare, on behalf of my coauthors, that the work described is original research that has not been published previously and is not under consideration for publication elsewhere, in whole or in part. All the authors listed have approved the manuscript that is enclosed.

## Authors Contributions

**Olin B. Jose** – Writing- review& editing, Writing – original draft, Visualization, Validation, Software, Methodology, Investigation, Conceptualization, Formal analysis, Data curation , **Manoharan A. N** – Investigation, Data curation, Formal analysis, Software, **A Krishnakumar**- Writing – review& editing, Writing – original draft, Visualization, supervision, Project administration, Funding acquisition, Conceptualization, **K Anoop Krishnan**-Writing-review&editing , Validation, Supervision, Methodology.

**Declaration of Human Participants**

This study did not involve live animal subjects or direct experimental intervention on humans. The research was based on chemical characterization of environmental samples and analysis of secondary, anonymized statistical data on cancer patients obtained legally through the Right to Information Act, 2005. Human health risks were assessed using established environmental exposure scenarios and risk assessment models; no human participants were enrolled or experimentally exposed. Therefore, this study did not require institutional ethical approval or individual informed consent.

**Refernces**


AI-Shawi, S. R. A., Kadhim, H. A. H., & Al-Saad, H. T. (2022). Assessment of heavy metals in exchangeable sediments samples from Tigris – Euphrates and Shatt al-Arab rivers. *Technology Audit and Production Reserves*, *6*(3(68)), 6–14. https://doi.org/10.15587/2706-5448.2022.267794

Al-Shammary, A. A. G., Al-Shihmani, L. S. S., Fernández-Gálvez, J., & Caballero-Calvo, A. (2024). Optimizing sustainable agriculture: A comprehensive review of agronomic practices and their impacts on soil attributes. *Journal of Environmental Management*, *364*, 121487. https://doi.org/10.1016/j.jenvman.2024.121487

Angon, P. B., Islam, Md. S., KC, S., Das, A., Anjum, N., Poudel, A., & Suchi, S. A. (2024). Sources, effects and present perspectives of heavy metals contamination: Soil, plants and human food chain. *Heliyon*, *10*(7), e28357. https://doi.org/10.1016/j.heliyon.2024.e28357

ATSDR. (2005). *Toxicological Profile for Zinc* (TP-60; p. 352). U.S. Department of health and Human Services , Agency for Toxic Substances and Disease Registry. https://www.atsdr.cdc.gov/toxprofiles/tp60.pdf

ATSDR. (2012). *Toxicological Profile for Vanadium* (TP-58; p. 255). U.S. Department of health and Human Services , Agency for Toxic Substances and Disease Registry. https://www.atsdr.cdc.gov/toxprofiles/tp58.pdf

ATSDR. (2020). *Toxicological Profile for Lead* (TP-13; p. 583). U.S. Department of health and Human Services , Agency for Toxic Substances and Disease Registry. https://www.atsdr.cdc.gov/toxprofiles/tp13.pdf

ATSDR. (2024a). *Toxicological Profile for Cobalt* (TP-33; p. 428). U.S. Department of health and Human Services , Agency for Toxic Substances and Disease Registry. https://www.atsdr.cdc.gov/toxprofiles/tp33.pdf

ATSDR. (2024b). *Toxicological Profile for Nickel* (TP-15; p. 10). U.S. Department of health and Human Services , Agency for Toxic Substances and Disease Registry. https://www.atsdr.cdc.gov/toxprofiles/tp15-c1.pdf

Bernal, J. P., Eggins, S. M., McCulloch, M. T., Grün, R., & Eggleton, R. A. (2006). Dating of chemical weathering processes by *in situ* measurement of U-series disequilibria in supergene Fe-oxy/hydroxides using LA-MC-ICPMS. *Chemical Geology*, *235*(1), 76–94. https://doi.org/10.1016/j.chemgeo.2006.06.009

Bland, W. J., & Rolls, D. (2016). *Weathering: An Introduction to the Scientific Principles* (0 ed.). Routledge. https://doi.org/10.4324/9781315824918

CGWB. (2007). *GROUND WATER INFORMATION BOOKLET OF KANNUR DISTRICT, KERALA STATE* (p. 36). CWRDM.

Conley, D. J. (2002). Terrestrial ecosystems and the global biogeochemical silica cycle. *Global Biogeochemical Cycles*, *16*(4), 68-1-68–8. https://doi.org/10.1029/2002GB001894

Cornu, S., Montagne, D., & Vasconcelos, P. M. (2009). Dating constituent formation in soils to determine rates of soil processes: A review. *Geoderma*, *153*(3), 293–303. https://doi.org/10.1016/j.geoderma.2009.08.006

Das, R., & Krishnakumar, A. (2022). Implications of Methane Emissions in Biogeochemical Budgeting: A Study from a Tropical Wetland System, Kerala, India. *Environmental Engineering Science*, *39*(2), 114–124. https://doi.org/10.1089/ees.2021.0121

De Corato, U., Viola, E., Keswani, C., & Minkina, T. (2024). Impact of the sustainable agricultural practices for governing soil health from the perspective of a rising agri-based circular bioeconomy. *Applied Soil Ecology*, *194*, 105199. https://doi.org/10.1016/j.apsoil.2023.105199

de Figueiredo, M. M. J. C., Guimarães, J. T. F., Salomão, G. N., Gastauer, M., Sahoo, P. K., da Silva, E. F., Reis, L. S., de Sousa, M. M., da Silva Junior, R. O., Martins e Souza-Filho, P. W., da Silveira Pereira, W. V., & Ramos, S. J. (2025). Geochemical thresholds and bioavailability of potentially toxic elements in Amazonian soils: A risk-based framework for environmental management in mineralized watersheds. *Environmental Advances*, *22*, 100667. https://doi.org/10.1016/j.envadv.2025.100667

Doran, J. W., & Zeiss, M. R. (2000). Soil health and sustainability: Managing the biotic component of soil quality. *Applied Soil Ecology*, *15*(1), 3–11. https://doi.org/10.1016/S0929-1393(00)00067-6

Duncan, A. E., de Vries, N., & Nyarko, K. B. (2018). Assessment of Heavy Metal Pollution in the Sediments of the River Pra and Its Tributaries. *Water, Air, & Soil Pollution*, *229*(8), 272. https://doi.org/10.1007/s11270-018-3899-6

Fausak, L. K., Bridson, N., Diaz-Osorio, F., Jassal, R. S., & Lavkulich, L. M. (2024). Soil health – a perspective. *Frontiers in Soil Science*, *4*. https://doi.org/10.3389/fsoil.2024.1462428

Fritsch, E., Morin, G., Bedidi, A., Bonnin, D., Balan, E., Caquineau, S., & Calas, G. (2005). Transformation of haematite and Al-poor goethite to Al-rich goethite and associated yellowing in a ferralitic clay soil profile of the middle Amazon Basin (Manaus, Brazil). *European Journal of Soil Science*, *56*(5), 575–588. https://doi.org/10.1111/j.1365-2389.2005.00693.x

Gadgil, M. (2011). *Report of the Western Ghats Ecology Expert Panel (WGEEP)*. Ministry of Environment and Forests, Government of India.

Gan, L., Wang, J., Xie, M., & Yang, B. (2022). Ecological risk and health risk analysis of soil potentially toxic elements from oil production plants in central China. *Scientific Reports*, *12*(1), 17077. https://doi.org/10.1038/s41598-022-21629-y

Gayathri, S., Dev, V. V., Raj, R. S., Krishnakumar, A., Maya, T. V., & Krishnan, K. A. (2021). Spatiotemporal evaluation of hydrochemical facies and pesticide residues in the cardamom plantations of Southern Western Ghats, India. *Environmental Nanotechnology, Monitoring & Management*, *16*, 100599.

Gayathri, S., Krishnan, K. A., Krishnakumar, A., Maya, T. M. V., Dev, V. V., Antony, S., & Arun, V. (2021). Monitoring of heavy metal contamination in Netravati river basin: Overview of pollution indices and risk assessment. *Sustainable Water Resources Management*, *7*(2), 20. https://doi.org/10.1007/s40899-021-00502-2

Gupta, H., Krishnakumar, A., & Krishnan, K. A. (2024). Multidimensional Approach for the Assessment of Environmental Pollution and Health Risk Associated With V, Ni, Cr, Cu, and Zn in the Recent Sediments of Kabini Interstate River, Southeastern Western Ghats, India. *Environmental Quality Management*, *34*(2), e22321. https://doi.org/10.1002/tqem.22321

Hakanson, L. (1980). An ecological risk index for aquatic pollution control.a sedimentological approach. *Water Research*, *14*(8), 975–1001. https://doi.org/10.1016/0043-1354(80)90143-8

Hoang, H. G., Hadi, M., Nguyen, M. K., Hai Nguyen, N. S., Huy Le, P. Q., Nguyen, K. N., Tran, H.-T., & Mishra, U. (2025). Assessing heavy metal pollution levels and associated ecological risks in peatland areas in the Mekong Delta region. *Environmental Research*, *274*, 121319. https://doi.org/10.1016/j.envres.2025.121319

Hoque, M. M., Islam, A., Islam, A. R. M. T., Pal, S. C., Mahammad, S., & Alam, E. (2023a). Assessment of soil heavy metal pollution and associated ecological risk of agriculture dominated mid-channel bars in a subtropical river basin. *Scientific Reports*, *13*(1), 11104. https://doi.org/10.1038/s41598-023-38058-0

Hoque, M. M., Islam, A., Islam, A. R. M. T., Pal, S. C., Mahammad, S., & Alam, E. (2023b). Assessment of soil heavy metal pollution and associated ecological risk of agriculture dominated mid-channel bars in a subtropical river basin. *Scientific Reports*, *13*(1), 11104. https://doi.org/10.1038/s41598-023-38058-0

Huang, J., Tian, Y., Liu, Z., Li, Z., Sun, S., Su, Z., & Dai, H. (2025). Contamination and source-specific health risk assessment of soil heavy metals in the middle and upper reaches of the Heihe River Basin of China. *Environmental Geochemistry and Health*, *47*(4), 92. https://doi.org/10.1007/s10653-025-02401-3

Idrus, F. A., & Ding, V. U. (2026). Heavy metal contamination in sediments of the Sematan-Serayan River, Sarawak: Assessment of pollution indices and environmental risk implications. *Environmental Monitoring and Assessment*, *198*(3), 253. https://doi.org/10.1007/s10661-026-15110-w

Kabato, W., Hailegnaw, N., Mutum, L., & Molnar, Z. (2025). Managing soil health for climate resilience and crop productivity in a changing environment. *Science of The Total Environment*, *1000*, 180460. https://doi.org/10.1016/j.scitotenv.2025.180460

Kakutey, K., Sackey, L. N. A., & Akoto, O. (2023). Impact of accumulation of copper from application of copper-based fungicides on soil properties in Ghana. *Discover Environment*, *1*(1), 1. https://doi.org/10.1007/s44274-023-00004-2

Kamunda, C., Mathuthu, M., & Madhuku, M. (2016). Health Risk Assessment of Heavy Metals in Soils from Witwatersrand Gold Mining Basin, South Africa. *International Journal of Environmental Research and Public Health*, *13*(7), 663. https://doi.org/10.3390/ijerph13070663

Kassa, H., Dondeyne, S., Poesen, J., Frankl, A., & Nyssen, J. (2017). Impact of deforestation on soil fertility, soil carbon and nitrogen stocks: The case of the Gacheb catchment in the White Nile Basin, Ethiopia. *Agriculture, Ecosystems & Environment*, *247*, 273–282. https://doi.org/10.1016/j.agee.2017.06.034

KILA. (2015). *Kuppam river Conservation master plan*.

Kiruba, T., Jayaprakash, P., Juliet Josephine Joy, J., Venkatamuthukumar, J., Suresh Gandhi, M., & Ravisankar, R. (2025). Assessment of metal contamination in sediment of Kerala Coast, India using EDXRF technique and Multivariate Statistical method. *Nuclear Analysis*, *4*(1), 100151. https://doi.org/10.1016/j.nucana.2024.100151

Kopittke, P. M., Menzies, N. W., Wang, P., McKenna, B. A., & Lombi, E. (2019). Soil and the intensification of agriculture for global food security. *Environment International*, *132*, 105078. https://doi.org/10.1016/j.envint.2019.105078

Kowalska, J. B., Mazurek, R., Gąsiorek, M., & Zaleski, T. (2018). Pollution indices as useful tools for the comprehensive evaluation of the degree of soil contamination–A review. *Environmental Geochemistry and Health*, *40*(6), 2395–2420. https://doi.org/10.1007/s10653-018-0106-z

Krishnakumar, A., Aditya, S. K., Krishnan, K. A., Vivekanandan, N., Kaliraj, S., & Jose, J. (2022). *Establishment of Baseline Reference Geochemical Values in Tropical Soils of Western Ghats: Assessment of Periyar Basin with Special Reference to Contaminant Geochemistry*. https://doi.org/10.1002/clen.202200382

Krishnakumar, A., Aditya, S. K., Seenipandi, K., Krishnan, K. A., & Jose, J. (2021). Evaluation of suspended sediment concentration and heavy metal distribution in Ashtamudi Lake, a Ramsar site in the southwest coast of India using remote sensing and GIS techniques. In *Remote sensing of ocean and coastal environments* (pp. 251–275). Elsevier. https://www.sciencedirect.com/science/chapter/edited-volume/pii/B9780128196045000159

Krishnakumar, A., Nair, G., Krishnan, K. A., Maya, T. M. V., & Jose, O. B. (2025). Geochemical and geospatial assessment of Tamiraparani river, draining through Kanyakumari, India—the gateway of sunrise and sunset: Insights into environmental pollution and sustainability. *Environmental Earth Sciences*, *84*(9), 252. https://doi.org/10.1007/s12665-025-12265-6

KSRRC, & KSPB. (2023). *Kuppam Priority-V*.

Kumar, S. & Anshumali. (2025a). Heavy metal pollution and health risk assessment in upland and riparian soils of the Ganga River basin. *Discover Soil*, *2*(1), 33. https://doi.org/10.1007/s44378-025-00061-4

Kumar, S. & Anshumali. (2025b). Heavy metal pollution and health risk assessment in upland and riparian soils of the Ganga River basin. *Discover Soil*, *2*(1), 33. https://doi.org/10.1007/s44378-025-00061-4

Lal, R. (2012). Climate Change and Soil Degradation Mitigation by Sustainable Management of Soils and Other Natural Resources. *Agricultural Research*, *1*(3), 199–212. https://doi.org/10.1007/s40003-012-0031-9

Lal, R. (2025). Soil Degradation and Pollution as the Global Public Health Emergency. *Medical Research Archives*, *13*(5). https://doi.org/10.18103/mra.v13i5.6474

Li, J., Li, X., Wang, C., Liu, J.-Z., Gao, Z.-D., Li, K.-M., Tuo, X.-Y., & Zang, F. (2024). Pollution characteristics and probabilistic risk assessment of heavy metal(loid)s in agricultural soils across the Yellow River Basin, China. *Ecological Indicators*, *167*, 112676. https://doi.org/10.1016/j.ecolind.2024.112676

Luo, M., Vandeputte, D. J., Lievens, S., Li, G., Su, Y., Huysmans, M., Elskens, M., Baeyens, W., & Gao, Y. (2025). Understanding the availability of metals in agricultural soils and the impact of manure application. *Journal of Hazardous Materials*, *493*, 138386. https://doi.org/10.1016/j.jhazmat.2025.138386

Madibekov, A., Ismukhanova, L., Opp, C., Saidaliyeva, Z., Zhadi, A., Sultanbekova, B., & Kurmanova, M. (2023). Spatial Distribution of Cu, Zn, Pb, Cd, Co, Ni in the Soils of Ili River Delta and State Natural Reserve "Ili-Balkhash." *Applied Sciences*, *13*(10), 5996. https://doi.org/10.3390/app13105996

Mandal, B. K., & Suzuki, K. T. (2002). Arsenic round the world: A review. *Talanta*, *58*(1), 201–235.

Mao, H.-R., Cui, L.-F., Zhang, Z.-J., Xu, S., Liu, C.-Q., & Zhao, Z.-Q. (2022). Influence of Monsoon Climate on Chemical Weathering of Granitic Regoliths. *Global Biogeochemical Cycles*, *36*(5), e2022GB007362. https://doi.org/10.1029/2022GB007362

Mathew, S., & Radhika, R. (2022). STATUS OF HEAVY METAL CONTAMINATION IN MAJOR RIVERS OF KERALA, SOUTH INDIA – A REVIEW. *UTTAR PRADESH JOURNAL OF ZOOLOGY*, 23–31. https://doi.org/10.56557/upjoz/2022/v43i213207

Mgelwa, A. S., Ngaba, M. J. Y., Hu, B., Gurmesa, G. A., Mwakaje, A. G., Nyemeck, M. P. B., Zhu, F., Qiu, Q., Song, L., Wang, Y., Fang, Y., & Rennenberg, H. (2025). Meta-analysis of 21st century studies shows that deforestation induces profound changes in soil characteristics, particularly soil organic carbon accumulation. *Forest Ecosystems*, *12*, 100257. https://doi.org/10.1016/j.fecs.2024.100257

Miao, X., Hao, Y., Zhang, F., Zou, S., Ye, S., & Xie, Z. (2020). Correction to: Spatial distribution of heavy metals and their potential sources in the soil of Yellow River Delta: a traditional oil field in China. *Environmental Geochemistry and Health*, *42*(2), 709. https://doi.org/10.1007/s10653-019-00243-4

Middelburg, J. J., van der Weijden, C. H., & Woittiez, J. R. W. (1988). Chemical processes affecting the mobility of major, minor and trace elements during weathering of granitic rocks. *Chemical Geology*, *68*(3), 253–273. https://doi.org/10.1016/0009-2541(88)90025-3

Mishra, P., Ali, S., Kumar, R., & Shekhar, S. (2025). Global lead contamination in soils, sediments, and aqueous environments: Exposure, toxicity, and remediation. *Journal of Trace Elements and Minerals*, *14*, 100259. https://doi.org/10.1016/j.jtemin.2025.100259

Mittal, B., & Kaushik, P. (2026). Human health risk assessment of heavy metals in water and soil irrigated by the textile waste contaminated Dravyavati River based on USEPA guidelines. *Discover Public Health*, *23*(1), 797. https://doi.org/10.1186/s12982-026-02142-3

Mng'ong'o, M. E. (2026). Pollution indices and ecological risk assessment associated with potentially toxic elements in irrigation sediments of Usangu agro-ecosystem. *Environmental Challenges*, *24*, 101619. https://doi.org/10.1016/j.envc.2026.101619

Mohan, U., & Krishnakumar, A. (2022). Geochemistry pollution status and contamination assessment of potentially toxic metals from the sediments of a tropical river of Kerala, India. *Environmental Nanotechnology, Monitoring & Management*, *18*, 100692. https://doi.org/10.1016/j.enmm.2022.100692

Moldovan, A., Török, A. I., Kovacs, E., Cadar, O., Mirea, I. C., & Micle, V. (2022). Metal Contents and Pollution Indices Assessment of Surface Water, Soil, and Sediment from the Arieș River Basin Mining Area, Romania. *Sustainability*, *14*(13), 8024. https://doi.org/10.3390/su14138024

Muller. (1969). *INDEX OF GEOACCUMULATION IN SEDIMENTS OF THE RHINE RIVER*. *2*(3), 108–118.

Nair, K. M., Padmalal, D., & Kumaran, K. (2006). Quaternary Geology of South Kerala Sedimentary Basin – An Outline. *Journal of the Geological Society of India*, *67*(2), 165–179. https://doi.org/10.17491/jgsi/2006/670205

NRSC. (2026). *Bhuvan – Indian Geo-Platform of ISRO* [Map]. National Remote Sensing Centre.

Nziguheba, G., & Smolders, E. (2008). Inputs of trace elements in agricultural soils via phosphate fertilizers in European countries. *Science of The Total Environment*, *390*(1), 53–57. https://doi.org/10.1016/j.scitotenv.2007.09.031

Office of the Registrar General & Census Commissioner. (1982). *Census of India 1981: Final Population Totals, Series-10 (Kerala), Paper 3 of 1981*. Directorate of Census Operations, Kerala, Ministry of Home Affairs, Government of India.

Office of the Registrar General & Census Commissioner. (1991). *Census of India 1991: Primary Census Abstract (General Population)—Kerala (Series 12)*. Directorate of Census Operations, Kerala, Ministry of Home Affairs, Government of India.

Office of the Registrar General & Census Commissioner. (2001). *Census of India 2001: Primary Census Abstract, Kannur District (Series 33, Part XII)*. Directorate of Census Operations, Kerala, Ministry of Home Affairs, Government of India.

Office of the Registrar General & Census Commissioner. (2011). *District Census Handbook: Kannur—Series 33, Part XII-B (Primary Census Abstract)*. Directorate of Census Operations, Kerala, Ministry of Home Affairs, Government of India.

P, R. (2024). Environmental Impact Assessment on Noyyal River Basin Special Reference to Water Quality. *International Journal for Research in Applied Science and Engineering Technology*, *12*(3), 21–43. https://doi.org/10.22214/ijraset.2024.58719

Paatero, P. (1997). Least squares formulation of robust non-negative factor analysis. *Chemometrics and Intelligent Laboratory Systems*, *37*(1), 23–35. https://doi.org/10.1016/S0169-7439(96)00044-5

Paatero, P., & Tapper, U. (1993). Analysis of different modes of factor analysis as least squares fit problems. *Chemometrics and Intelligent Laboratory Systems*, *18*(2), 183–194. https://doi.org/10.1016/0169-7439(93)80055-M

Paatero, P., & Tapper, U. (1994). Positive matrix factorization: A non-negative factor model with optimal utilization of error estimates of data values. *Environmetrics*, *5*(2), 111–126. https://doi.org/10.1002/env.3170050203

Pescke, I. K., de Oliveira Rozino, L., & Vargas, V. M. F. (2026). Hydrological disturbance reshapes trace metal contamination and ecological risk through fine-sediment redistribution in subtropical river sediments. *Discover Geoscience*, *4*(1), 342. https://doi.org/10.1007/s44288-026-00692-2

Prasood, S. P., Mukesh, M. V., Sajinkumar, K. S., Srinivas, R., Lakshmi, R., Chrips, N. R., & Thrivikramji, K. P. (2024). Heavy metal load in waters and sediments of Karamana River Basin, southwestern India: A COVID-19 lockdown modulation. *Total Environment Advances*, *9*, 200089. https://doi.org/10.1016/j.teadva.2023.200089

Rajan, S., & Nandimandalam, J. R. (2024). Environmental health risk assessment and source apportion of heavy metals using chemometrics and pollution indices in the upper Yamuna river basin, India. *Chemosphere*, *346*, 140570. https://doi.org/10.1016/j.chemosphere.2023.140570

Reshma, C., & Arunkumar, R. (2023). Assessment of impact of climate change on the streamflow of Idamalayar River Basin, Kerala. *Journal of Water and Climate Change*, *14*(7), 2133–2149. https://doi.org/10.2166/wcc.2023.456

Rodríguez-Trejo, A., González-Guzmán, R., Ibarra-Ortega, H. E., Böhnel, H., Solís-Valdez, S., Rodríguez, R., Guzmán, G., & Castañeda-Miranda, A. G. (2026). Environmental magnetism and geochemical screening of anthropogenic contamination in suburban university campus topsoil: Lithogenic controls and localized ferrimagnetic

enrichment in Querétaro, Mexico. *Applied Geochemistry*, *211*, 107103. https://doi.org/10.1016/j.apgeochem.2026.107103

Rudnick, R. L., & Gao, S. (2003). 3.01—Composition of the Continental Crust. In H. D. Holland & K. K. Turekian (Eds.), *Treatise on Geochemistry* (pp. 1–64). Pergamon. https://doi.org/10.1016/B0-08-043751-6/03016-4

Sababa, E., Essomba Owona, L. G., Temga, J. P., & Ndjigui, P.-D. (2021). Petrology of weathering materials developed on granites in Biou area, North-Cameroon: Implication for rare-earth elements (REE) exploration in semi-arid regions. *Heliyon*, *7*(12), e08581. https://doi.org/10.1016/j.heliyon.2021.e08581

Shepard, D. (1968). A two-dimensional interpolation function for irregularly-spaced data. *Proceedings of the 1968 23rd ACM National Conference, ACM '68*, 517–524. https://doi.org/10.1145/800186.810616

Siji, S., Krishnakumar, A., Nair, G., & Krishnan, K. A. (2025). Geochemistry and contamination metrics of the tropical agricultural soils in Karuvannur Basin, India, with special reference to environmental sustainability. *Environmental Geochemistry and Health*, *47*(11), 513. https://doi.org/10.1007/s10653-025-02832-y

Soman, k. (2023). *Geology of Kerala*. Geological Society of India. https://books.google.com/books/about/Geology_of_Kerala.html?id=1llPAQAAIAAJ

Sun, X., Wang, H., Guo, Z., Lu, P., Song, F., Liu, L., Liu, J., Rose, N. L., & Wang, F. (2020). Positive matrix factorization on source apportionment for typical pollutants in different environmental media: A review. *Environmental Science: Processes & Impacts*, *22*(2), 239–255. https://doi.org/10.1039/c9em00529c

Taylor, S., & McLennan, S. (1985). The Continental Crust: Its Composition and Evolution. *Department of Geosciences Faculty Publications*. https://commons.library.stonybrook.edu/geo-articles/12

Tomlinson, D. L., Wilson, J. G., Harris, C. R., & Jeffrey, D. W. (1980). Problems in the assessment of heavy-metal levels in estuaries and the formation of a pollution index. *Helgoländer Meeresuntersuchungen*, *33*(1–4), 566–575. https://doi.org/10.1007/BF02414780

USEPA. (1989). *Risk Assessment Guidance for Superfund (RAGS), Volume I: Human Health Evaluation Manual (Part A)* (EPA/540/1-89/002). Office of Emergency and Remedial Response.

USEPA. (2011). *Exposure Factors Handbook: 2011 Edition* (Nos. 978-0-16-089180–2). National Center for Environmental Assessment.

USEPA, O. (2026). *Regional Screening Levels (RSLs)—User's Guide* [Data and Tools]. https://www.epa.gov/risk/regional-screening-levels-rsls-users-guide

Vandana, M., John, S. E., Maya, K., & Padmalal, D. (2020). Environmental impact of quarrying of building stones and laterite blocks: A comparative study of two river basins in Southern Western Ghats, India. *Environmental Earth Sciences*, *79*(14), 366. https://doi.org/10.1007/s12665-020-09104-1

Wang, D., Tian, F., Yang, M., Liu, C., & Li, Y.-F. (2009). Application of positive matrix factorization to identify potential sources of PAHs in soil of Dalian, China. *Environmental Pollution, Special Issue Section: Ozone and Mediterranean Ecology: Plants, People, Problems*, *157*(5), 1559–1564. https://doi.org/10.1016/j.envpol.2009.01.003

Wang, X., Wan, S., Clift, P. D., Zhao, D., Cai, G., Yang, Y., Zhang, J., Yu, Z., Jin, H., Song, Z., Tang, Y., Zhang, S., & Li, A. (2025). Human Activities Induced Stronger Silicate Weathering in the Red River Basin: A Growing Carbon Sink During the Late Holocene. *Journal of Geophysical Research: Earth Surface*, *130*(10), e2025JF008433. https://doi.org/10.1029/2025JF008433

Wang, Y., Xu, W., Li, J., Song, Y., Hua, M., Li, W., Wen, Y., Li, T., & He, X. (2022). Assessing the fractionation and bioavailability of heavy metals in soil–rice system and the associated health risk. *Environmental Geochemistry and Health*, *44*(2), 301–318. https://doi.org/10.1007/s10653-021-00876-4

*Water Atlas of Kerala*. (1995). Centre for Water Resources Development and Management.

Wei, H., Niu, X., Li, M., Cui, C., Wei, Z., Long, W., Tang, M., Yu, H., Zhang, P., He, L., & Pan, B. (2024). Potentially toxic element source apportionment and risk assessment in agricultural soils around a large-scale Pb-Zn mine in

Southwest China. *Journal of Environmental Chemical Engineering*, *12*(5), 113722. https://doi.org/10.1016/j.jece.2024.113722

Wieczorek, J., Baran, A., & Bubak, A. (2023). Mobility, bioaccumulation in plants, and risk assessment of metals in soils. *Science of The Total Environment*, *882*, 163574. https://doi.org/10.1016/j.scitotenv.2023.163574

Wu, Y., Wang, Y., & Xie, X. (2014). Spatial occurrence and geochemistry of soil salinity in Datong basin, northern China. *Journal of Soils and Sediments*, *14*(8), 1445–1455. https://doi.org/10.1007/s11368-014-0874-8

Yang, E., Wang, Q., Zhang, Z., Shao, W., Luo, H., Xiao, X., Ni, F., Mi, J., Sun, X., & Guan, Q. (2024). Source-oriented health risk assessment of heavy metals in a soil-river continuum in northwest China. *International Journal of Sediment Research*, *39*(6), 916–928. https://doi.org/10.1016/j.ijsrc.2024.09.001

Yang, S., Huang, Q., Lv, Y., Zhou, X., Hou, M., & Bao, Y. (2026). Geochemical differences and sources of mineral elements in soil and coffee beans from pu'er and Baoshan, China. *BMC Plant Biology*, *26*(1), 1160. https://doi.org/10.1186/s12870-026-08998-6

Zou, Z., Tan, S., & Yang, Z. (2026). Assessment of heavy metal contamination in Yellow River Delta surface soils: Spatial distribution, sources, ecological risks, and probabilistic health implications. *Environmental Geochemistry and Health*, *48*(9), 404. https://doi.org/10.1007/s10653-026-03304-7

## Supplementary Files

This is a list of supplementary files associated with this preprint. Click to download.

- SupplementaryTable1.docx